

REVIEWER #1

This study evaluates a Keeling-style approach for determining the deuterium-excess signature of combustion derived water vapor (CDV) in the Salt Lake City area. The new approach is consistent with values reported in the group's earlier paper, Gorski et al., 2015. The paper also develops criteria for filtering observational periods when atmospheric conditions are most conducive to the accumulation of CDV. These criteria could be used as a starting point for similar studies conducted in other cities. This is the first study that reports multiple years of water vapor isotope measurements to study CDV. While the study is certainly novel, and the quantification of CDV is important, I think the authors could improve the paper by (1) explicitly stating why this study is important using detailed examples, (2) discussing the broader impacts of the work (how does this work further the field, and where else are improvements needed), and (3) providing quantitative support to put the results of the study into context. For example, the reasons some parameter values are used (e.g. emission factors (ef) from 1-2, CDV mole fractions ranging from 100-500 ppm) should be supported with more explanation. The paper is well-written and concise. The specific suggestions listed below, if incorporated, will provide readers with greater context for interpreting the results of the study.

Specific Comments:

- 1. Pg. 1. Ln 21. This might be the only sentence in the paper that explicitly states why quantifying CDV emissions is important. Could you expand this idea by detailing possible CDV impacts in urban areas, e.g. impacts on downwind clouds/weather, link between enhanced humidity/temperatures and heat stroke/fatalities in at-risk groups (elderly, sick), influence on photochemistry/aerosol, etc.**

This is a great suggestion – we've added a few sentences at this point to expand on the complex relationships between CDV, atmospheric stability and meteorology, and potential impacts for human health. This section now reads (pg 2, L. 1-7):

In turn, water vapor from fossil fuel combustion may impact urban air quality and meteorology, including through direct changes in radiative balance by increased water vapor concentrations (Holmer and Eliasson, 1999; McCarthy et al., 2010), impacts on aerosols and cloud properties (Pruppacher and Klett, 2010; Mölders and Olson, 2004; Kourtidis et al., 2015; Twohy et al., 2009; Carlton and Turpin, 2013; Kaufman and Koren, 2006), and altered local or downwind precipitation amounts (Rosenfeld et al., 2008). Where combined with atmospheric stratification, these changes can potentially lengthen or intensify periods of elevated particulate pollution in cities, which would directly impact public health through increased incidence of acute cardiovascular (Morris et al., 1995; Brook et al., 2010) or respiratory (Dockery and Pope, 1994) illness.

- 2. Pg. 2. Ln 11. This is an appropriate place to introduce the idea of the SLV's seasonally shifting fossil fuel use (and H₂O:CO₂ combustion stoichiometry), which adds to the complexity of quantifying CDV emissions. Furthermore, fossil fuel use trends differ from city to city. Describing the complexities of (1) CDV isotope measurements and (2) uncertainties regarding stoichiometry, fossil fuel**

consumption, and the impacts on CDV d-excess and emissions estimates bolsters your statements regarding the need for refinements to the method (last sentence of abstract). It would also help to communicate the novelty of these types of studies, and the need to continue work in this area.

To address this comment, we have added a new section (section 2) between the introduction and methods section that describes fossil fuel use in the SLV and outlines stoichiometric relationships between CDV and CO₂ in emissions. We hope that this section both provides additional context necessary for this study, but also provides some useful guidelines for how to estimate emissions factors for other cities. This section forms page 3 and L1-4 of page 4 in the revised manuscript.

- 3. Pg. 2. Ln 16-19. The last line of the introduction indicates that an objective of this study is to investigate relationships involving CDV amount. Does your analysis allow you to report CDV contributions to the SLC boundary layer (Gorski et al reports up to 13% CDV), or do you mean to say your approach allows for the estimation of CDV mole fractions (based on CDV moistening lines in Figure 1, 7-9), or do you mean to say this study intends to report general relationships between atmospheric stability and CDV amount (not necessarily quantitative estimates). Please clarify.**

The most direct approach for us to follow is the first one suggested by the reviewer. In our initial submission, we did not make quantitative estimates as there were large uncertainties in d_{CDV} . The revised approach for estimating e_f suggested in this revision allows for a more meaningful estimation of the CDV contribution.

We've clarified the goals of this study in the last paragraph of the introduction (L. 23-31 of P. 2), and added sections and tables to the results examining CDV amount relationships.

- 4. Pg 3 ln 4. Why is 2200 msl used in the VHD equation? Is it because that's roughly the height of the mountains surrounding the SLV? Or does it have to do with average mixing height (1290 m + 1500 m = 2790 m, so maybe not?)**

The column integral ends at 2200 m ASL because this is roughly the elevation of the Oquirrh Mountain ridgeline bounding the west end of the SLV. Whiteman et al. (2014) also suggested this elevation as it maximizes the correlation between the VHD metric and PM_{2.5} concentrations. We have added a sentence indicating that the upper bound of this summation arises from the height of the Oquirrh Mountains:

The upper bound in the VHD calculation (2200 m) is determined by the elevation of the Oquirrh Mountain ridgeline, which forms the western valley boundary.

- 5. Pg 3. Ln 6. You reference Whiteman et al., 2014 for the PCAP definition, but more explanation of Whiteman et al.'s 4.04 MJ/m² number would be useful.**

We have added a few sentences here to provide context for this 4.04 MJ/m² threshold (P5, L. 7-

10):

This VHD threshold of 4.04 MJ/m² corresponds to the mean VHD in days where the SLV daily fine particulate matter concentration (PM_{2.5}) exceeds half of the US National Ambient Air Quality Standard for PM_{2.5} (17.5 μg m⁻³) (Whiteman et al. 2014). This threshold has been used in subsequent studies of SLV air quality and atmospheric stability (Baasandorj et al., 2017; Bares et al., 2018), and we have retained this convention for intercomparison with prior studies.

6. Pg 3. Ln 23. What were the dD and d18O values of the standards, and did they bracket the range of observed delta values?

Four standards were used throughout this period of record, with a swap in standards made on February 16, 2017 (e.g., the new standards only apply to the last ~10 measurement days of this study. A summary table is provided below:

	Prior to February 16, 2017		After February 16, 2017	
	δ ¹⁸ O	δ ² H	δ ¹⁸ O	δ ² H
Light standard	-16.0	-121.0	-15.88	-199.66
Heavy standard	-1.23	-5.51	1.65	16.9

They did not bracket the range of observed delta values, but we have reason to believe that the potential uncertainty introduced by this situation is small as the Picarro instruments are extremely linear. Internal measurements of VSLAP, which has isotopic compositions of -55.50‰ for δ¹⁸O and -427.5‰ for δ²H, are within a few tenths of a permil of the values predicted using a calibration based on these standards despite a notably lighter isotopic composition that is significantly lighter than any vapor observed in our study.

7. Pg 3 Ln 28 / Section 2.2. Please comment on the reproducibility of the calibrations and robustness of the calibration correction. Is it a linear or non-linear correction, both (over certain [H2O] ranges)? There is also no statement regarding instrument precision in the deltas. There is no statement about uncertainty analysis for d-excess (as a function of water vapor concentration). Figure 10 is the only part of the paper that indicates an uncertainty analysis was conducted.

We have revised this section of the manuscript to more explicitly describe uncertainties in the data and in our data processing routines, and to provide an estimate of analytical precision. This section has been revised to read as follows (P5. L30 to P6, L12):

Calibration of raw instrument values at ~1 Hz on the instrument scale to hourly averages on the VSMOW scale proceeds across three stages: (1) Measured isotope values are corrected for an apparent dependence on cavity humidity, using correction equations developed by operating the standards delivery module at a range of injection rates, corresponding to cavity humidity values from 500-30000 ppm. Instrumental precision is determined in this step, with uncertainties arising both from a decrease in instrument precision with decreasing cavity humidity, and uncertainty in the regression equation to correct for this bias. The humidity correction is determined by a linear

regression of the deviation of isotopic composition from the measured isotopic composition at a reference humidity against the inverse of cavity humidity. The reference humidity used is 15,000-25,000 ppm, which is the typical humidity that liquid water samples are measured and at which the lab standards are calibrated. Additional details on this correction are provided in a supplement. (2) Analyzer measurements are calibrated to the VSMOW-VSLAP scale using two standards of known isotopic composition delivered by the standards delivery module, using calibration periods that bracket a series of ambient vapor measurements to correct for analytical drift, (3) corrected measurements were aggregated to an hourly time step. Measurement uncertainties are primarily limited by changes in instrument precision with cavity humidity, and 1σ uncertainties range from 0.88‰ for $\delta^{18}\text{O}$, 3.61‰ for $\delta^2\text{H}$, and 7.93‰ for d-excess at 1,000 ppm; to 0.14‰ for $\delta^{18}\text{O}$, 0.53‰ for $\delta^2\text{H}$, and 1.24‰ for d-excess at 10,000 ppm.

Additional details, as well as plots of our correction showing the decrease in precision with decreases in humidity, are included as a supplement.

- 8. Pg. 5. Ln 28. What amount of fossil fuel (for CH₄ for example) would be required to produce 500 ppm CDV? It would be helpful to provide this information to put the numbers into context. Figure 1 shows isohumes from 100-500 ppmv, but I don't know if this range of CDV is what contributes to the SLV boundary layer on average or if it's an upper limit estimate. You could frame this in the context of CO₂ emissions. Hestia CO₂ is available for SLC, so you could estimate what average CDV mole fractions would be on a non-PCAP day (using $ef = 1-2$), and then make estimates of PCAP CDV contributions assuming 24+ hours of emissions accumulate within a lower (average observed PCAP) boundary layer.**

Following the estimated ef value for SLV estimated using the HESTIA dataset and described in our response to point #2 above, we have added a sentence here that translates these CDV concentrations into equivalent CO₂ increases (P.8, L.7-8):

Assuming a representative ef value of 1.5 (section 2), 100 or 500 ppm of CDV correspond to CO₂ increases of 66.7 or 333.3 ppm, respectively.

- 9. Pg. 6. Ln. 4. What are the expected ef values, and why?**

We've added a section on likely ef by fuel source in our revisions and found that a reasonable SLV-scale ef value for SLV winter of 1.5. Emissions factors can range from ~0.5-2 though, depending on fuel source, as described in section 2 of our revised manuscript (see point #2). We've clarified our approach to ef in this regression by adding the following sentence (P. 8, L. 17-19):

The ef parameter depends on the molar ratios of hydrogen to carbon in the fuel source; we estimate a fuel-source-weighted SLV-scale ef value for winter of 1.5, but note that ef values for hydrocarbon fuels can vary from $< 0.5 - 2$.

- 10. Pg. 6. Ln 9. What type of linear fitting routine is used here? There is error in the x**

and y variables presumably, which should be accounted for in the fitting.

It is true that there is measurement error in both x and y. The x component is calculated as a difference of two CO₂ measurements, which each have an estimated uncertainty associated with them of 0.1 ppm. Assuming the errors in these two measurements are uncorrelated, the net uncertainty in the measurements on the x-axis are approximately 0.14 ppm, or 1.4×10^{-4} mmol/mol. We estimate that error in the y-axis is primarily determined from the isotope measurement uncertainties, which depend on humidity and range from 1.2‰ at 10000 ppm H₂O to 7.9‰ at 1000 ppm H₂O. Based on this formulation, the y error is >8500x larger than the x error; therefore, we suggest that ordinary least squares fitting is sufficient here.

11. Pg. 7. Ln 10. Again, cross correlations were determined with what kind of fitting routine? There is error in both x and y, although in this case, the error would be much higher in d- excess than CO₂. It also would be useful to report in a table the correlations observed during PCAP periods and non-PCAP periods in addition to those reported for the four winters.

We're a little confused by this comment, as measures of correlation are not sensitive to measurement error. We calculated cross-correlation values using the Pearson definition of the correlation coefficient as the covariance of x and y at lag τ divided by the product of the standard deviations of x and y:

$$\rho_{xy}(\tau) = \frac{\text{cov}(x, y)(\tau)}{\sigma_x \sigma_y}$$

Neither of these values are sensitive to normally-distributed measurement error, and therefore, the cross-correlation value should not be sensitive to differences in measurement error between x and y. This result is in contrast to regression slopes and intercepts, which are sensitive to differences in measurement error between x and y, as typical least-squares regression assumes that all of the measurement error is contained within y.

12. Pg. 9 ln. 4. During PCAP events, is there an average observed decrease in d-excess per ppm increase in CO₂? What magnitude of CO₂ enhancement is required to observe a change in d-excess (at the d-excess LOD)?

This is essentially the slope of the linear model presented in Figure 6, following an appropriate scaling of the x-axis from mmol/mol to ppm or $\mu\text{mol/mol}$. The slope of the best-fit linear mixed model is -268 ± 26 (‰ mmol H₂O)/mmol CO₂, which corresponds to a slope of -179 ± 17 ‰ / mmol CO₂ assuming the emissions factor of 1.5 that we determined from the HESTIA emissions inventory. This suggests a $\sim 0.18 \pm 0.02$ ‰ decrease in d-excess for every ppm increase in CO₂. Assuming a 1σ uncertainty of d-excess of 2.4‰ at 4 mmol/mol humidity (a representative mean DJF value for the SLV), and a considering a 2σ change to be the LOD, we estimate a ~ 27 ppm enhancement of CO₂ is required to see a measurable change in d-excess.

We have added the following sentences detailing this analysis to the end of this section, after we present the regression results in figure 6 (P. 12, L. 21-25):

Based on this regression, we estimate that d-excess decreases by $0.18 \pm 0.02\%$ for every ppm increase in CO_2 . Instrumental precision (1σ) for d-excess is estimated to be 2.4% at the mean DJF humidity value of 4 mmol/mol, implying that enrichments of ~ 40 ppm CDV can be detected at the 2σ level. This estimated detection limit will likely decrease as instrument precision and calibration routines are improved.

13. Pg. 9 Ln 12. What about the deposition of vapor to a snow or ice-covered surface when RH w.r.t. ice is 100%. In the presence of ice/snow, would the deposition of vapor result in drier air with a more negative d-excess value? This effect would be more important at night as temperatures fall?

This is an interesting possibility that we did not discuss in the initial submission. Deposition of snow or ice would have opposing impacts on vapor d-excess depending on whether deposition is occurring at saturation or at supersaturation. Vapor deposition at $\text{RH} = 100\%$ should raise d-excess, not lower it (e.g., Figure 1 and Galewsky et al., 2011; Jouzel & Merlivat, 1984), but vapor deposition at supersaturation would introduce a kinetic effect that would lower vapor d-excess relative to its equilibrium value at saturation (e.g., Galewsky et al., 2011; Jouzel & Merlivat, 1984). We don't have any direct observations of supersaturation but cannot rule out the possibility of supersaturation on snow surfaces or during cloud formation.

If kinetic isotope fractionation during vapor deposition were responsible for the observed decreases in d-excess, we might expect to see temporal coherence between decreases in specific humidity and decreases in d-excess. Instead, we see little change in d-excess overnight while q is decreasing, but strong decreases in d-excess associated with increases in CO_2 in the early morning (revised Fig. 10, attached to our response to point 17 below).

We've haven't made any changes to the manuscript at this point in the methods, but have included this possibility as a discussion point (see our response to comment #19 below).

14. Pg. 9 Ln 28-30. This is true, but the measurements you present were all from winter months. There is EIA fossil fuel consumption data available which provides information about the distribution of fossil fuel types consumed for regions in the US at monthly(?) resolution. You surely can make some educated guess about the fossil fuel consumption- weighted emission factor for SLC during winter months.

In our revised version, we've used the emission estimates from the HESTIA dataset (Gurney et al., 2012; Patarasuk et al., 2016) and a simplifying assumption about the fuels corresponding to each sector used in the HESTIA dataset in order to make a more informed estimate of the $\text{H}_2\text{O}:\text{CO}_2$ emissions factor. We find that an ef value of 1.5 is appropriate based on the distribution of fuel use across Salt Lake County. We also reassessed our model selection and found more support for a model allowing a random effect in both the slope and intercept. The best fit slope in the new model with an ef of 1.5 is $-179 \pm 17\%$.

In light of these changes, we've revised these sentences at pg. 9, L. 24-30 to read (in revised MS, this section is at p. 12, l. 17-21):

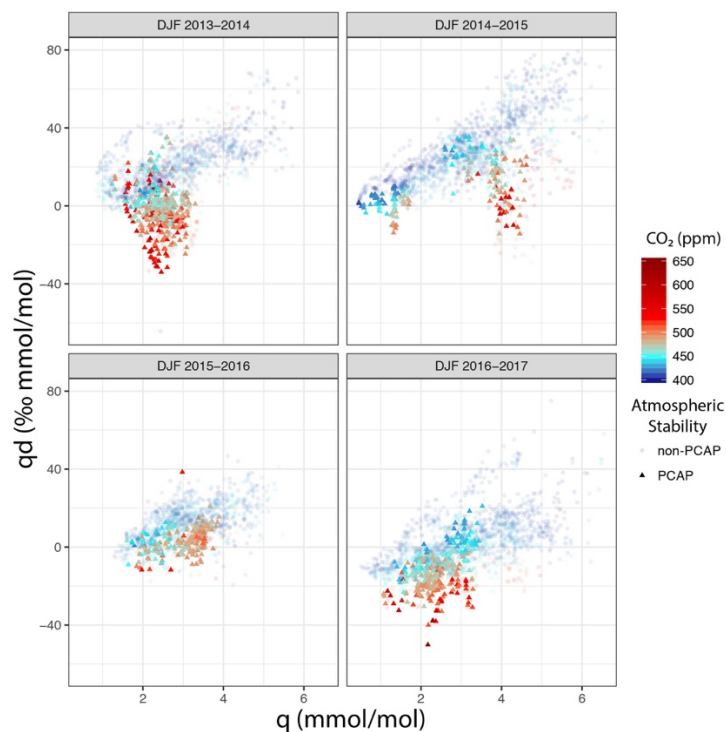
The best-fit slope of a linear mixed model allowing for random variation in the slope and intercepts across PCAP events yields an estimate of d_{CDV} of $-179 \pm 17\%$ (assuming $ef = 1.5$). This estimate of d_{CDV} is consistent with the upper limit of the theoretical estimates and pilot measurements from Gorski et al. (2015), and could be validated by a comprehensive survey of fuels in the SLV.

We have also changed the appropriate section of the methods to reflect this change in model selection (pg 8, L 21-30):

We apply two linear mixed models where PCAP-to-PCAP event-scale variability is treated as a random effect to estimate d_{CDV} : in the first, the slope is assumed to be constant across all PCAP events but the intercept is allowed to vary, while in the second, both the slope and intercept are allowed to vary across PCAP events. These models are constructed to find the best-fit slope, and therefore the best-fit estimate of d_{CDV} , across all PCAP events. As a result, they implicitly assume that changes in d_{CDV} through time are small compared to changes in $d_{bg}q_{bg}$, or that changes in the emissions profile of SLV are small compared to environmental variability in humidity and d-excess. We consider only the second model in our results as we find it has more support than the first model, with this selection determined based on lower AIC and BIC scores for the second model.

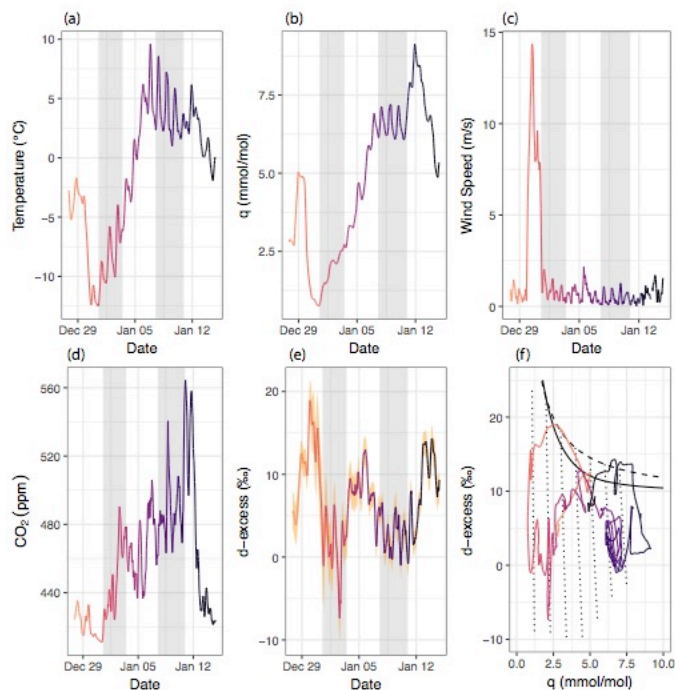
15. Pg. 11 Fig 5. It is difficult to distinguish between the circles and squares in Figure 5. Could you try larger markers, or filled vs unfilled markers, or circles vs crosses?

We have revised this figure to change the opacity of the circles and squares to help distinguish between PCAP and non-PCAP periods. PCAP periods are high-opacity triangles, while non-PCAP periods are low-opacity circles. These changes have made this figure significantly more readable. The revised figure has been pasted below.



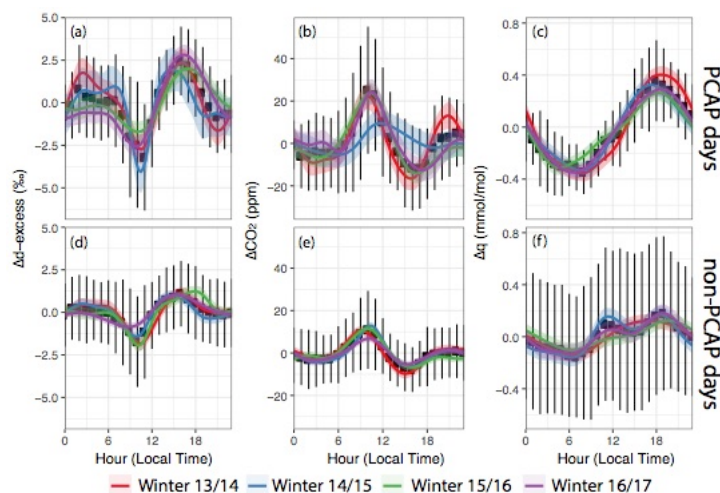
16. Pg. 14 Fig 7 (and Figures 8, 9). Can you change the color scale to one that goes from red- purple. It would be easier to distinguish the PCAP periods in the (a) d-excess vs q plots where the PCAP observations track with the CDV moistening lines.

The color scale of figures 7 and 8 have been changed to one that spans orange-red-purple, as suggested. Figure 9 and its associated section has been removed following a suggestion from reviewer #2, and to keep the manuscript concise in light of the added sections on combustion stoichiometry and uncertainty analysis. We have also changed the panels in these plots to be (a) temperature, (b) specific humidity, (c) wind speed, (d) CO₂ concentration, (e) d-excess, (f) qd vs q to help clarify relationships between CO₂, d-excess, and q. The revised figure 7 is included below to illustrate these changes.



17. Pg. 20 Figure 10 caption. This is the first time that measurement uncertainty is discussed. You report that the shading reflects the standard error, but there is no quantitative discussion of d-excess uncertainty. This should appear in the Methods.

We have revised our manuscript to include a more systematic error analysis, and clarify sources of error (e.g., measurement based, or arising from uncertainty in the regressions). The error shown in our original submission was the standard error of the regression, not of the data underlying the regression. To make the uncertainty in the diurnal cycles more apparent, we have revised figure 10 to include information on data uncertainty. Mean values for each hour across all four years are shown as a black dot, with 1σ variability shown as a vertical black line. As in the initially submitted version, lines show a GAM estimation of the diurnal cycle to show differences in the diurnal cycle across years, with shading indicating the standard error of the model fit. We have updated the figure caption to reflect these changes, and the revised figure is pasted below.



A quantitative discussion of d-excess uncertainty has been added to the methods and is detailed in our response to comment #7 above.

18. Pg. 21 ln 7. This is an indicator that this phenomenon is difficult to observe (even in SLC). This would be an appropriate place to discuss whether the CDV d-excess measurement precision is good enough to observe CDV d-excess in other cities (that may be naturally more humid).

We view this result as likely reflecting the changing footprint integrated by these measurements, and that the heating emissions were more likely kept lower in the valley. We've added a sentence here that clarifies that this relationship might be more strongly observed elsewhere in the valley, as diurnal cycles of CO_2 are also more pronounced elsewhere in the valley (e.g., Mitchell et al., 2018) (P. 23, L. 6-11):

Average diurnal cycles in d-excess and CO_2 showed little change overnight outside of PCAP events (Fig. 10), which was unexpected as heating emissions continued throughout the evening. The absence of overnight d-excess and CO_2 changes was likely a result of the UOU's location on a topographic bench away from large residential areas, or due to injection of cleaner air from above if a surface-based inversion occurs at an elevation below the UOU site. Long-term records of CO_2 have also been collected in lower-elevation areas of the SLV and exhibit a greater buildup of CO_2 overnight during the winter (e.g., Mitchell et al., 2018), which suggests that a stronger trend in nighttime d-excess and CO_2 values might be observed elsewhere in the SLV.

We have also added a paragraph to the end of the discussion providing some guidance as to where else this technique might be useful (P. 24, L. 25-33):

This technique for measuring water from combustion in urban areas can be adapted beyond the SLV, though different environments will present distinct challenges. The SLV is well-suited to detecting the buildup of CDV as it has a dry climate, features a large urban area in a topographic basin, and experiences frequent multi-day periods of high atmospheric stability in the winter. The CDV signal is largest in dry regions or during winter (Fig. 1), and CDV may comprise a

larger fraction of urban humidity in these cities for a given level of emissions intensity. However, though the CDV signal is higher at low humidities, instrumental precision is lower. Therefore, at current instrumental precision limits, there is a trade-off between precision of the CDV estimates and the size of the CDV signal.

19. Pg 21. Ln 19-20. This is a repeat of one of my comments above, but what about deposition of vapor in ice supersaturated conditions? Is there snow on the ground during this study period? I think this would impart a more negative d-excess value in the remaining vapor.

Based on our revised figure 10, which includes diurnal cycles in specific humidity, we view the potential role of vapor deposition under supersaturation to be small, but we cannot rule it out. We consider this possibility to have a likely small impact as we see a much closer association in diurnal cycles of d-excess with diurnal cycles of CO₂ than of q (Fig. 10, pasted below). Nonetheless, this is a really interesting possibility and we cannot rule it out – we have added the following sentences to this section (P. 23, L. 25-30):

Deposition of vapor onto ice in supersaturated conditions can also promote a decrease in vapor d-excess (Galewsky et al., 2011; Jouzel & Merlivat, 1984). While we do not have any direct observations of supersaturated conditions, we cannot rule out the possibility of supersaturated conditions occurring when snow is in the valley or during cloud formation. However, we expect that any potential role for vapor deposition under supersaturated conditions on vapor d-excess to be small, as we do not typically observe decreases in d-excess concurrent with decreases in specific humidity (Fig. 10).

20. Pg. 21. Ln 24. This is another repeat of one of my earlier comments. I think reporting CDV d-excess ranges are fine for $ef=1$ or $ef=2$, but I think you could also make an educated guess based on Patarasuk et al., 2016, EIA, and other literature to say if you believe ef is closer to 1 or 2 (probably closer to 1?). This shows that the community needs information about the partitioning of the fossil fuels consumed in various cities, at the very least at seasonal resolution.

We have taken this suggestion and made a quantitative estimate of ef for winter Salt Lake County using the HESTIA data set (Gurney et al., 2012; Patarasuk et al., 2016). We provide a most likely estimate of 1.5 as a valley-scale ef value. A more detailed answer to this point is provided above in our responses to points 8 and 9.

In light of this, we have rephrased this sentence as follows (P. 23, L. 31-34):

We have made an estimate of 1.5 for ef through a detailed accounting of emissions or fuel sources from the HESTIA dataset (Patarasuk et al., 2016), but several sources of uncertainty in net ef remain. For example, heat exchangers designed to improve heating efficiency may reduce the H₂O concentration in emissions, and potentially alter d_{CDV} as well through condensation of water in the emissions stream (Fig. 1).

21. Pg. 22. Ln 2. What type of refinements?

This sentence has been moved to the last paragraph of the discussion, and has been expanded as follows (P.23, L. 31 to P. 23, L. 9):

However, though the CDV signal is higher at low humidities, instrumental precision is lower. Therefore, at current instrumental precision limits, there is a trade-off between precision of the CDV estimates and the size of the CDV signal. Based on our study, we suggest two potential refinements to this technique that will improve the accuracy and precision of this technique to diagnose the fraction of urban humidity arising from CDV. First, the largest source of known uncertainty in our estimates is associated with d_{CDV} . While our estimate of $-179 \pm 17\%$ is consistent with theoretical estimates, this fraction may vary through time as a result of changing fuel mixtures (affecting both isotopic composition and ef) or measurement footprints, and has not been rigorously validated with direct measurements of d_{CDV} from a wide variety of fuel sources and combustion systems. Additionally, due to spatial variability in the $\delta^2\text{H}$ composition of fuels, d_{CDV} likely varies for other cities. Second, the estimate of the urban CDV fraction of humidity is highly sensitive to the estimate of d_{bg} . In this study, estimates of the CDV humidity percentage were 2.2% greater on average when a low CO_2 threshold was used rather than one based on the time window immediately preceding the PCAP; in one case, these assumptions yielded estimates that varied by a factor of 3.4, and in other cases, even yielded different signs (Table 3). In our uncertainty analysis, we have considered uncertainty arising from instrumental precision, but the uncertainty in d_{bg} remains difficult to assess. Paired urban-rural observations may be necessary to accurately estimate d_{bg} , or identify appropriate periods for estimating d_{bg} from the urban record.

22. Pg 22 Ln 8. The statement regarding the lack of a robust relationship b/n CDV or CO_2 and mixing height refers to the entire wintertime period, or just PCAP events?

We've removed this sentence as it could be read ambiguously and the rest of the paragraph conveys our point here. A true quantitative relationship between mixing height and CDV/ CO_2 amounts is difficult to evaluate with the data we have for a few reasons: (a) atmospheric soundings at the airport occur before sunrise and around sunset every day, and therefore, are unable to capture diurnal changes in mixing height well, and (b) the build-up of CO_2 and CDV in the boundary layer requires prolonged stability, not just stability. In this view, evaluating the relationship between current mixing height and CO_2 may be misleading.

23. Pg. 22 Conclusions. The single conclusions paragraph is essentially a summary. Please provide a discussion about the impacts of your work from a broader perspective. Can these studies only be done in wintertime in semi-arid environments? What refinements would advance this science? Where are improvements needed?

We have revised our conclusion to address these points, in accordance with the suggested revisions. The new conclusion reads as follows (p. 24, L.10 – p.25, L. 6):

Measurements of ambient vapor d-excess were paired with CO₂ observations across four winters in Salt Lake City, UT. We found a strong negative association between CO₂ and d-excess on sub-diurnal to seasonal timescales. Elevated CO₂ and CDV was most prominent during PCAP periods, where atmospheric stability was high for extended periods. We outline theoretical models that can discriminate between changes in d-excess driven by condensation, advection, and mixing processes the “natural” hydrological cycle and those driven by CDV moistening. The CDV signal is largest when humidity is low, as CDV likely comprises a larger fraction of total humidity and the anticipated signal between vapor with and without CDV is large. On shorter timescales, prominent diurnal cycles were observed in both d-excess and CDV that could be tied to both emissions intensity and atmospheric processes. These diurnal cycles were decoupled from diurnal cycles of specific humidity, further strengthening the link between d-excess and urban CO₂.

We estimate the d-excess value of CDV to be $-179 \pm 17\text{‰}$ assuming a mean molar ratio of H₂O:CO₂ in emissions of 1.5 derived from the HESTIA inventory of emissions for Salt Lake County (Patarasuk et al., 2016; Gurney et al., 2012). This estimate is consistent with theoretical constraints and a limited number of direct observations of CDV (Gorski et al., 2015), though uncertainty remains due to variability in the valley-scale stoichiometric ratio of H₂O and CO₂ and the measurement footprint, and uncertainties about the isotopic composition of fuels and their transit through different combustion systems. The latter of these uncertainties can be reduced in future studies that seek to generate a “bottom-up” estimate of d_{CDV} from direct measurements of fuels and emissions vapor to complement the “top-down” estimate made in this study using a mixing-model approach. We use our d_{CDV} estimate to calculate the fraction of humidity in the SLV comprised of CDV using two different assumptions for the d-excess of water vapor in the absence of fossil fuel emissions. We find that CDV generally represents 5-10% of urban humidity during PCAP events, with a maximum estimate of $16.7 \pm 3.2\%$. Estimates of urban CDV fraction require an accurate estimate of the d-excess of water vapor in the absence of emissions, and we find generally higher estimates of urban CDV when a low-CO₂ threshold is used to estimate d_{bg} compared to when pre-PCAP observations alone are used. Further refinements of these methods may help apportion humidity changes during the winter between CDV and different advected “natural” water sources to the urban environment, and help verify that CO₂ measurements that are taken as backgrounds are not influenced by local emissions. Additionally, our method is most immediately applicable to cities in arid or semi-arid areas during the winter, as the potential isotopic signal for detecting CDV is the largest. However, CDV may have the largest impact on urban meteorology when humidity is low, as greenhouse forcing by water vapor is logarithmically proportional to water vapor concentration. Further refinements of this humidity apportionment technique, such as narrowing the uncertainty in the isotopic composition of CDV and improving the estimation of d_{bg} will improve estimates of CDV amount in urban environments, and help assess relationships between CDV, CO₂, urban air pollution, and public health.

Technical Corrections:

1. Pg 2. Ln 3. VSMOW abbreviation not defined

We have defined “VSMOW” prior to its first use on page 2 in the revised version.

2. Pg 2. Ln 6. “produce” not “product”?

We were referring to reaction products here, but recognize this sentence was needlessly ambiguous and confusing. We have revised this sentence to read:

The reaction of ^{18}O -enriched oxygen with ^2H -depleted fuels produces vapor with an unusually negative deuterium excess value ($d = \delta^2\text{H} - 8\delta^{18}\text{O}$; Dansgaard, 1964) that is distinct in the “natural” hydrological cycle.

3. Pg 2 Ln 33. VHD abbreviation should appear on previous line after first instance of “valley heat deficit”

We have made this change.

4. Pg 4. Ln 3. Meteorological*

This typo has been corrected.

5. Pg. 13 ln 25. Remove “a” between “likely” and “due”

This typo has been corrected.

REVIEWER #2 – Dr. Ingeborg Levin

Review of the manuscript by Fiorella et al. “Detection and variability of combustion-derived vapor in an urban basin”

General Remarks:

The manuscript presents follow-up work and an extension of continuous observations of co-located measurements of atmospheric CO₂ mole fraction and deuterium excess in atmospheric water vapor to investigate the impact of combustion-derived water vapor (CDV) at a monitoring station in the Salt Lake City basin in Utah, USA, during winter. The particularly low deuterium excess values of CDV significantly influence the isotopic signature of atmospheric water vapor during inversion situations at cold temperatures when atmospheric humidity is generally low and during stable weather conditions when combustion-derived emissions (CO₂ and H₂O) accumulate in the atmospheric boundary layer. The authors estimate, in a Keeling-style mixing model approach, the range of CDV d-excess values, which turns out to be large. They claim that these results could be used to constrain contributions of combustion to urban humidity and meteorology (Abstract), or possibly verify CO₂ emissions amounts and/or emissions reductions (Conclusions).

From their four-year observations, the authors convincingly show that the isotopic signature of atmospheric water vapor can be significantly modified by CDV during winter, but I am not convinced that there is a realistic chance to use the observed relation between high CO₂ and low d-excess in atmospheric water vapor in a quantitative way. As discussed by the authors, the variability of combustion material and its large range of H₂O/CO₂ stoichiometry when burned to CO₂ and H₂O as well as potential isotope effects during production and emission strongly modify d-excess of CDV. Furthermore, not all CO₂ emissions during winter can be solely associated with combustion processes, but some CO₂ emissions may also originate from biogenic sources that are not associated with net H₂O emissions. Therefore, the constraints on urban humidity and CO₂ emissions mentioned in the Abstract and Conclusions, to my understanding are not justified. A sensitivity study including a thorough uncertainty analysis would be required to support these optimistic statements.

In view of the weaknesses of the “tracer” CDV d-excess, I think the manuscript is too detailed. It has too many figures showing similar, mainly semi-quantitative, features that make the manuscript unnecessarily lengthy. For example, I am not sure that all three case studies (described in Figures 7, 8, 9) need to be presented and discussed in detail. Figure 7 would be sufficient to convince the reader that the processes introduced before really take place and are visible in the observations. In addition, Figures 4, 5 and 6 give somewhat redundant information, with Figure 5, to me, being the most convincing. Figure 4 more or less summarizes what is visible in detail in the time series shown in Figure 3, and Figure 6 somehow “hides” the large variability in the Keeling plots, that are expected because the signature of CDV is not well defined and variable in time. I am missing the error analysis that quantifies the ranges of d-excess and emission factors stated.

Technical: (1) There are many abbreviations used in the manuscript (VHD, PCAP, WBB, SDM, ...), which are new for the reader. It would very much help to spell them out again if they had not been used for a while.

We've revised the text to remove abbreviations that are infrequently used (e.g., SBI, SDM, etc.) – abbreviations that are frequently used remain.

(2) Please note that CO₂ concentrations are also calibrated as micromole per mole (or ppm), but not ppmv (Fig. 7, 8, 9).

We've changed all instances of ppmv to ppm to avoid confusion.

Specific Remarks:

Introduction, first sentence: please give reference.

We have clarified here that this is estimated from carbon emissions as follows (pg. 1, L. 18-20):

Fossil fuel combustion releases carbon dioxide and water to the atmosphere. Annual carbon emissions are estimated to be 9.5 Pg C/y (Le Quéré et al., 2018), which suggests annual water emissions from combustion of ~21.1 Pg, assuming a mean molar ratio of H₂O:CO₂ in emissions of 1.5 (section 2, and also Gorski et al., 2015).

Page 2 line 5: “produce”;

We were referring to reaction products here, but recognize this sentence was needlessly ambiguous and confusing. We have revised this sentence to read:

The reaction of ¹⁸O-enriched oxygen with ²H-depleted fuels produces vapor with an unusually negative deuterium excess value ($d = \delta^2\text{H} - 8\delta^{18}\text{O}$; Dansgaard, 1964) that is distinct in the “natural” hydrological cycle.

line 16: “from”

Good catch – thanks. This typo has been corrected.

Page 3 Eq. (1): why sum up to 2200 m?

The column integral ends at 2200 m asl because this is roughly the elevation of the Oquirrh Mountain ridgeline bounding the west end of the SLV. Whiteman et al. (2014) also suggested this elevation as it maximizes the correlation between the VHD metric and PM_{2.5} concentrations. We have added a sentence indicating that the upper bound of this summation arises from the height of the Oquirrh Mountains (pg. 5, L. 5-6):

The upper bound in the VHD calculation (2200 m) is determined by the elevation of the Oquirrh Mountain ridgeline, which forms the western valley boundary.

line 22: how long was the tubing and was it heated (e.g. to avoid condensation effects)?

The sampling tubing was ~10 m long (half indoors) and was not heated. We observed no condensation in the tubing, and observed no periods of unusual bias between humidity values measured by the Picarro CRDS and the meteorological station.

line 25: give reference to script.

A link to the processing scripts is provided in the code and data availability section of this manuscript.

Page 4 line 2: how often was calibrated? measurements uncertainties?

Calibrations were performed every 12 hours, with two standard waters being measured for at least 15 minutes each. Measurement uncertainties are primarily limited by changes in instrument precision with cavity humidity, and 1σ uncertainties range from 0.88‰ for $\delta^{18}\text{O}$, 3.61‰ for $\delta^2\text{H}$, and 7.93‰ for d-excess at 1000 ppm; to 0.14‰ for $\delta^{18}\text{O}$, 0.53‰ for $\delta^2\text{H}$, and 1.24‰ for d-excess at 10000 ppm.

We have added this information to the methods section (pg. 6, L. 2-12), and have included plots detailing how uncertainties change with humidity as a supplement.

line 3: “meteorological”;

This typo has been corrected.

line 27: is the time shift between ASB and WBB taken into account in the pre-2014 data?

We did not shift the ASB data, as the time magnitude of the shift was small and the measurement period where these observations overlapped did not cover an entire annual cycle. We’ve added the following sentence to clarify this point (pg. 7, L. 3-5):

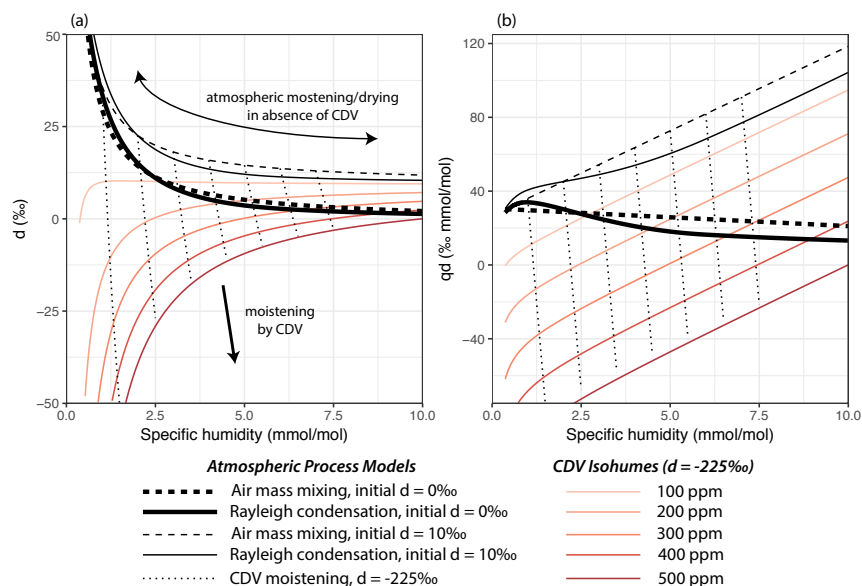
We do not adjust the ASB time series as the potential time shift is small, and the period of overlapping records is short and does not span a full annual cycle.

line 28: better spell out CDV in the title.

We have made this change.

Page 6 Fig. 1: the yellow line is not well visible;

We have revised figure 1 to use a gradient of reds to make the 100 ppm CDV isohume more visible. The revised figure is copied here as well.



line 1: is the total ΔCO_2 from combustion processes, i.e. no flux from biosphere?

For Salt Lake City, the biogenic contribution to ΔCO_2 has been shown to be negligible compared to the anthropogenic flux (Pataki et al., 2003, 2006, 2007; Strong et al., 2011). We have added the following sentence to this paragraph to clarify this point (pg. 8, L. 20-23):

Observations of urban $\delta^{13}\text{C}\text{-CO}_2$ and atmospheric modeling of the SLV indicate that wintertime increases in CO_2 above background concentrations are driven by anthropogenic emissions, and that the contribution from local respiration to urban CO_2 enhancement is likely negligible (Pataki et al., 2003, 2005, 2007; Strong et al., 2011).

line 2: subscripts “obs”

Good catch – this typo has been corrected.

Page 7 Fig. 2 and line 6: In the figure (mixing heights) ground level starts at 0 m while in the text total heights in m a.s.l. are reported; this is confusing

We have revised the sentence at line 6 to express heights in meters above ground level, making this sentence consistent with Fig. 2:

Calculated mixing heights ranged from the surface (0 m AGL) to 3390 m AGL, with a median value of 270 m AGL.

Page 9 line 6: is the correlation really “strong” and does this Figure provide new information compared to Fig. 3?

We agree that Figure 4 in our original submission did not provide any data that was not already presented in Figures 3 or 5.

Therefore, we have removed this figure in our revisions.

lines 10-14: in Fig. 5, qd is plotted vs. q , the text explanations are thus unclear.

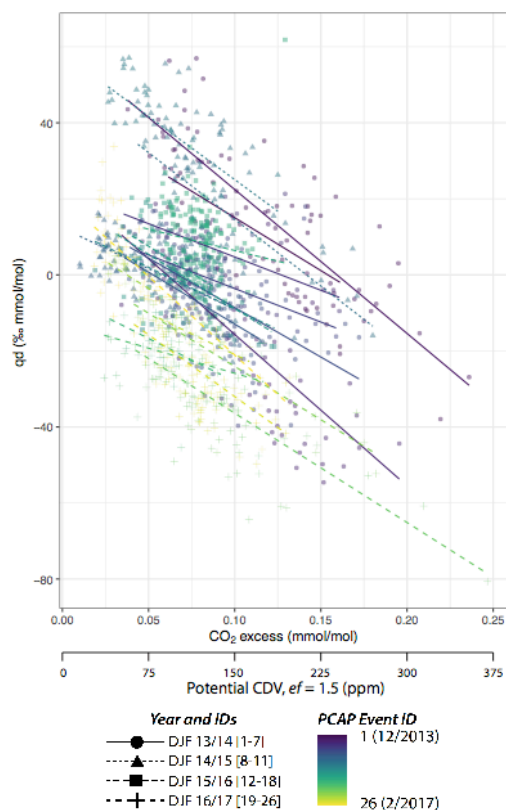
Good catch – we've revised this section to read as follows to indicate we're analyzing a plot of qd vs q :

Changes in the product of q and d-excess relative to q from atmospheric moistening and drying processes in the absence of CDV are expected to follow a linear relationship with a positive slope (Fig. 1). In contrast, addition of CDV to the atmosphere will promote strong, linear, and negative-sloped deviations from this qd - q relationship that are proportional to the amount of CDV. These patterns are observed in our measurements, where qd values trend up with q at low CO_2 concentrations, and decrease linearly with increasing CO_2 (Fig. 5).

Page 12 Figure 6: would like to see single events here to better judge on the significance of the correlation (see general comment concerning the significance of the Keeling approach to estimate end members)

We have taken several steps to hopefully improve our implementation of the Miller-Tans formulation of the Keeling approach, described below:

- 1) *We have gone back and assessed whether the model in the original submission represents the best model formulation. We have determined that it was not. Our original submission featured a linear-mixed model, where a random effect across PCAP events was allowed in the intercept. In our revisions, we have discovered that a model fit allowing for random effects in both the slope and intercept across PCAP events has more support via lower AIC and BIC scores. To illustrate this change, we have provided a revised figure 6 and revised text in the methods (pg 8, L. 23-30):*



We apply two linear mixed models where PCAP-to-PCAP event-scale variability is treated as a random effect to estimate d_{CDV} : in the first, the slope is assumed to be constant across all PCAP events but the intercept is allowed to vary, while in the second, both the slope and intercept are allowed to vary across PCAP events. These models are constructed to find the best-fit slope, and therefore the best-fit estimate of d_{CDV} , across all PCAP events. As a result, they implicitly assume that changes in d_{CDV} through time are small compared to changes in $d_{bg}q_{bg}$, or that changes in the emissions profile of the SLV are small compared to environmental variability in humidity and d-excess. We consider only the second model in our results as we find it has more support than the first model, with this selection determined based on lower AIC and BIC scores for the second model.

- 2) *We have provided summary statistics (e.g., slope with regression uncertainty and an R^2 value) for the Keeling approach as a supplementary table for each individual PCAP event using a more simple, linear ordinary least squares model (Table 2, pg. 15).*
- 3) *Following suggestions from reviewer #1, we have made a more quantitative estimate of the ef parameter to narrow the ranges of d_{CDV} estimated through this regression. To generate an improved estimate of ef, we used the HESTIA data set (Patarasuk et al., 2016), which is a bottom-up emissions inventory at hourly and building-scale resolution and breaks down emissions by economic sector. We estimate that at the valley scale, an emissions weighted ef value of 1.5 is appropriate. (Section 2, pg. 3 to pg. 4, L. 4).*

Page 13: please give times as local station time or in UTC; panels in Figure 7 (and 8, 9) seem to have been mixed up and do not correspond to the text. As d-excess is shown only in relation with moisture (and not vs. time), it is difficult to see the temporal correlations between CO₂ and d. Perhaps add a seventh panel.

The times provided are in UTC; we have changed “Z” to UTC to clarify this.

Pages 15-18: please explain why it is important to discuss these two case studies.

We sought to investigate compare a few different PCAP scenarios, and how the d-excess and CO₂ timeseries coevolved under different conditions. However, in light of the expanded discussion on SLV fuel sources and stoichiometry and the additional uncertainty analysis, we have removed the third case study presented in our initial submission for brevity. We have decided to retain the first two as they show different patterns, with the former showing a strong coupling between d-excess and CO₂, and the latter illustrating a period where though there is strong diurnal variability between d-excess and CO₂, changes in specific humidity seem to be largely driven by other factors.

Page 19 line 7: what is MST?

MST is “Mountain Standard Time,” the local time. To avoid confusion, and in accordance with ACP author recommendations, we have changed all instances of “MST” to “LT” to indicate local time vs. UTC.

Page 20 Fig. 10: uncertainties hardly visible

We’ve made three changes to Figure 10 to help interpret the uncertainty in these panels. First, we’ve made the uncertainties in the GAM fits more prominent to better show the error in the model fits. Second, we’ve added a layer to this plot indicating the variability in the data these models are constructed on. Mean hourly Δd -excess and ΔCO_2 values are shown as black dots with 1σ variability shown as vertical lines. Third, as differences across months are small, we have plotted these quantities as seasonal averages instead of monthly averages.

In response to comments raised by reviewer #1, we’ve also added a column in this figure showing the diurnal cycle of specific humidity. The above steps to clarify uncertainty are also extended to this column.

Page 21 lines 6-8: Maybe WBB is generally not well located on the topographic bench; what is SBI?

We’ve clarified the role of the WBB on the topographic bench here, and how it may contribute to the patterns we observe over night (pg. 22, L. 5-11):

Average diurnal cycles in d-excess and CO₂ showed little change overnight outside of PCAP events (Fig. 8), which was unexpected as heating emissions continued throughout the evening. The absence of overnight d-excess and CO₂ changes was likely a result of the UOU’s location on

a topographic bench away from large residential areas, or due to injection of cleaner air from above if a surface-based inversion occurs at an elevation below the UOU site. Long-term records of CO₂ have also been collected in lower-elevation areas of the SLV and exhibit a greater buildup of CO₂ overnight during the winter (e.g., Mitchell et al., 2018), which suggests that a stronger trend in nighttime d-excess and CO₂ values might be observed elsewhere in the SLV.

Page 22 lines 2 and 26-27: this seems to me far from realistic – please justify and make an uncertainty estimate (see general comments)

After consideration, we agree that this conclusion is too optimistic. Instead, we suggest that water isotope observations may be useful to help validate whether CO₂ observations that are taken to represent “background” values, as background CO₂ values should not be significantly correlated with water vapor d-excess if these CO₂ values are not influenced by local emissions. We have revised the sentence at line 2 to read (in revised MS, pg. 23 L. 33 to pg. 24 L. 9):

Based on our study, we suggest two potential refinements to this technique that will improve the accuracy and precision of this technique to diagnose the fraction of urban humidity arising from CDV. First, the largest source of known uncertainty in our estimates is associated with d_{CDV} . While our estimate of $-179 \pm 17\text{‰}$ is consistent with theoretical estimates, this fraction may vary through time as a result of changing fuel mixtures (affecting both isotopic composition and ef) or measurement footprints, and has not been rigorously validated with direct measurements of d_{CDV} from a wide variety of fuel sources and combustion systems. Additionally, due to spatial variability in the $\delta^2\text{H}$ composition of fuels, d_{CDV} likely varies for other cities. Second, the estimate of the urban CDV fraction of humidity is highly sensitive to the estimate of d_{bg} . In this study, estimates of the CDV humidity percentage were 2.2% greater on average when a low CO₂ threshold was used rather than one based on the time window immediately preceding the PCAP; in one case, these assumptions yielded estimates that varied by a factor of 3.4, and in other cases, even yielded different signs (Table 3). In our uncertainty analysis, we have considered uncertainty arising from instrumental precision, but the uncertainty in d_{bg} remains difficult to assess. Paired urban-rural observations may be necessary to accurately estimate d_{bg} , or identify appropriate periods for estimating d_{bg} from the urban record.

And the final sentence at lines 26-27 to read (in revised MS, pg. 25, L. 4-6):

Further refinements of this humidity apportionment technique, such as narrowing the uncertainty in the isotopic composition of CDV and improving the estimation of d_{bg} will improve estimates of CDV amount in urban environments, and help assess relationships between CDV, CO₂, urban air pollution, and public health.

Detection and variability of combustion-derived vapor in an urban basin

Richard P. Fiorella¹, Ryan Bares², John C. Lin^{2,3}, James R. Ehleringer^{4,3}, and Gabriel J. Bowen^{1,3}

¹Department of Geology and Geophysics, University of Utah, 115 S 1460 E, Salt Lake City, UT, 84112, USA

²Department of Atmospheric Sciences, University of Utah

³Global Change and Sustainability Center, University of Utah

⁴Department of Biology, University of Utah

Correspondence to: Richard Fiorella (rich.fiorella@utah.edu)

Abstract. Water emitted during combustion may comprise a significant portion of ambient humidity (>10%) in urban areas, where combustion emissions are strongly focused in space and time. Stable water vapor isotopes can be used to apportion measured humidity values between atmospherically transported and combustion-derived water vapor, as ~~combustion~~ combustion-derived vapor possesses an unusually negative deuterium excess value (d-excess, $d = \delta^2H - 8\delta^{18}O$). We investigated the relationship between the d-excess of atmospheric vapor, ambient $\text{CO}_2\text{-CO}_2$ concentrations, and atmospheric stability across four winters in Salt Lake City, UT. We found a robust inverse relationship between $\text{CO}_2\text{-CO}_2$ excess above background and d-excess on sub-diurnal to seasonal timescales, which was most prominent during periods of strong atmospheric stability that occur during Salt Lake City winter. ~~We developed a framework for partitioning changes in water vapor d-excess between advective changes in vapor and the addition of combustion-derived vapor.~~ Using a Keeling-style mixing model approach, and assuming a molar ratio of H_2O to CO_2 in emissions of 1.5, we estimated the d-excess of ~~combustion~~ derived combustion-derived vapor in Salt Lake City to be ~~between -125% and -308% broadly consistent with $-179 \pm 17\%$,~~ consistent with the upper limit of theoretical estimates. Based on this estimate, we calculate that vapor from fossil fuel combustion often represents 5-10% of total urban humidity, with a maximum estimate of 16.7%, consistent with prior estimates for Salt Lake City. Moreover, our analysis highlights that changes in the observed d-excess during periods of high atmospheric stability cannot be explained without a vapor source possessing a strongly negative d-excess value. Further refinements in ~~our~~ estimate of the isotopic composition of combustion-derived vapor require constraints on valley-scale stoichiometry between CO_2 and H_2O in combustion products, yet our results demonstrate the utility of stable water vapor isotopes to constrain contributions of combustion to this humidity apportionment method, most notably empirical validation of the d-excess of combustion vapor or improvements in the estimation of the background d-excess value in the absence of combustion, can yield more certain estimates of the impacts of fossil fuel combustion on urban humidity and meteorology.

1 Introduction

Fossil fuel combustion releases ~~~ 10 of water vapor~~ carbon dioxide and water to the atmosphere. Annual carbon emissions are estimated to be 9.4 Pg C y^{-1} (Le Quéré et al., 2018), which suggests annual water emissions from combustion of 21.1 Pg ,

assuming a mean molar emissions ratio between $\text{H}_2\text{O}:\text{CO}_2$ of 1.5 (section 2, and also Gorski et al., 2015). This water flux is negligible in the hydrologic cycle on global and annual timescales (e.g., Trenberth et al., 2006), but it may be significant to urban hydrologic cycling and meteorology as fossil fuel emissions are tightly concentrated in space and time (Bergeron and Strachan, 2012; Duren and Miller, 2012; Gorski et al., 2015; Sailor, 2011; Salmon et al., 2017). In turn, water vapor from fossil fuel combustion may ~~have subsequent impacts on~~ impact urban air quality and meteorology. ~~However,~~ including through direct changes in radiative balance by increased water vapor concentrations (Holmer and Eliasson, 1999; McCarthy et al., 2010), impacts on aerosols and cloud properties (Pruppacher and Klett, 2010; Mölders and Olson, 2004; Kourtidis et al., 2015; Twohy et al., 2009; Carlton et al., 2009), and altered local or downwind precipitation amounts (Rosenfeld et al., 2008). Where combined with atmospheric stratification, these changes can potentially lengthen or intensify periods of elevated particulate pollution in cities, which would directly impact public health through increased incidence of acute cardiovascular (Morris et al., 1995; Brook et al., 2010) or respiratory (Dockery and Pope, 1994) illness. However, using standard meteorological measurements it remains difficult to partition humidity from isolate combustion-derived vapor (CDV) from “naturally-occurring” ~~or advected water vapor using standard meteorological measurements, making its impact~~ water vapor, or vapor from other anthropogenically-influenced fluxes (e.g., snow sublimation from buildings), making the impact of CDV on the urban atmosphere difficult to assess.

Stable water vapor isotopes represent a promising method to ~~apportion~~ partition observed water vapor between combustion and advection sources (Gorski et al., 2015). Combustion of hydrocarbons produces water from the reaction of atmospheric oxygen, which is ^{18}O -enriched relative to ~~VSMOW~~ the international standard, Vienna Standard Mean Ocean Water (VSMOW) (+23.9 ‰, Barkan and Luz, 2005), and structurally-bound fuel hydrogen, which is ^2H -depleted relative to VSMOW due to preference for ^1H over ^2H during biosynthetic reactions (e.g., Estep and Hoering, 1980; Sessions et al., 1999). The reaction of ^{18}O -enriched oxygen with ^2H -depleted fuels ~~imparts~~ produces vapor with an unusually negative deuterium excess value ($d = \delta^2\text{H} - 8\delta^{18}\text{O}$; Dansgaard, 1964) to product vapor ($d = \delta^2\text{H} - 8\delta^{18}\text{O}$; Dansgaard, 1964) that is distinct compared to d-excess value in the “natural” hydrological cycle. Deuterium excess is ~ 10 ‰ ~~on average, on average,~~ in precipitation (Dansgaard, 1964; Rozanski et al., 1993), and ranges in “natural” waters from +150-200 ‰ in vapor in the upper troposphere (Blossey et al., 2010; Bony et al., 2008; Webster and Heymsfield, 2003) to ~ -60 ‰ in highly evaporated surface waters (e.g., Fiorella et al., 2015). In contrast, Gorski et al. (2015) estimated CDV d-excess values for fuels in Salt Lake Valley (SLV) ranging from -180 to -470 ‰, depending on the isotopic composition of the fuel and the degree of equilibration of oxygen isotopes between ~~CO_2 and H_2O~~ CO_2 and H_2O in combustion emissions.

The ~~SLV forms a basin, within which the~~ Salt Lake City, UT metro area (population of ~ 1.15 million) is located within the SLV. The SLV ($\sim 1300 - 1500$ m) is bounded on the west by the Oquirrh Mountains ($\sim 2200 - 2500$ m), on the east by the Wasatch Mountains (>3000 m), and on the south by the Traverse Mountains (< 2000 m). The northwest corner of the basin is bounded by the Great Salt Lake. During the winter, cold air often pools in the SLV, increasing atmospheric stability and limiting transport of combustion products away ~~from~~ from the city and impairing air quality. Previous work in the SLV indicated that CDV comprised up to $\sim 13\%$ of urban specific humidity during strong inversion events in winter 2013-2014 (Gorski et al., 2015). Here we combine those data with three additional winters of water vapor isotope measurements in Salt Lake City, UT (DJF 2014-2017) ~~; allowing us to investigate relationships between meteorology, atmospheric stability, to refine~~

our estimate of the d-excess of CDV, update estimates of the contributions of CDV to the urban atmosphere, and identify the largest sources of error that can be addressed or reduced in future studies.

2 Stoichiometric relationships between CO₂ and CDV and fuel use in SLV

5 The ratio of CO₂ to CDV in fossil fuel emissions depends on the stoichiometry of the fuels used. The chemical reaction for the idealized combustion of a generic hydrocarbon is:



10 The molar ratio of H₂O and ~~estimated CDV amount~~ CO₂ in product vapor is defined here as the emissions factor (*ef*), and arises directly from the molar ratio of hydrogen and carbon in the fuel as $y/2x$. Of simple hydrocarbons, methane (CH₄) has the greatest *ef* value of 2. Longer-chained hydrocarbons, such those in gasoline, have lower *ef* values. Octane (C₈H₁₈) has an *ef* value of 1.125, for example (Gorski et al., 2015).

15 Fuels burned within the SLV are generally petroleum products and natural gas, with the latter being extensively used in the winter for residential heating. Seasonal patterns of fuel use emerge from both "top-down" and "bottom-up" style emissions estimates. A high-resolution, bottom-up, building-level emissions inventory has been produced for Salt Lake County as part of the HESTIA project (Gurney et al., 2012; Patarasuk et al., 2016; Zhou and Gurney, 2010). On an annual basis, onroad transport represents 42.9% of Salt Lake County emissions, followed by the residential (20.8%) and industrial (12.6%) sectors (Patarasuk et al., 2016). The commercial, electric generation, and non-road transport sectors comprise the remaining 23.7% of Salt Lake County emissions. In winter, however, the residential sector is a much larger contributor to Salt Lake County emissions (34.4%), followed by the onroad transport (34.3%) and commercial sectors (13.1%) (Table 1). The remaining 18.2% of emissions arise from the non-road transport, electricity production, and industrial sectors. The increased prominence of residential and commercial sector emissions during the winter, primarily at the expense of onroad and industrial emissions, likely results from a greater heating demand and a concomitant increase in natural gas use. "Top-down" observations of stable carbon isotope compositions in atmospheric CO₂ in the SLV reflect this seasonal change in carbon inputs from primarily from gasoline combustion and respiration in the summer to a much stronger signal from natural gas in the winter (Pataki et al., 2003, 2005).

25 From these considerations, we estimate a valley-scale *ef* value using the HESTIA emissions inventory (Patarasuk et al., 2016) and appropriate emissions factors for natural gas, petroleum, and sub-bituminous coal resources. Natural gas was assumed to be composed of 90% methane, 8% ethane, and 2% propane (Schobert, 2013), yielding an *ef* value of 1.95. Petroleum products such as gasoline, jet fuel, and fuel oil, were assumed to be 85% C and 15% H by mass (Schobert, 2013; Dabelstein et al., 2012), yielding an *ef* value of 1.05. Finally, an *ef* value of 0.5 was assigned to coal, assuming a molar ratio of hydrogen to carbon of 1 (Schobert, 2013). Fuels or fuel mixtures were assigned to each economic sector in the HESTIA data set (Table 1). Mobile emissions (airport, on road, non-road, and railroad) were assigned petroleum sources, while the residential and electricity generation sectors were assigned natural gas sources (Table 1). Coal combustion supplies the majority of electricity in Utah and in SLV, but the power plants supplying the SLV are outside of the valley to the south. Electricity generation facilities

Table 1. HESTIA Emissions Estimates and estimated ef values for Salt Lake County

<u>Economic sector</u>	<u>December</u>	<u>January</u>	<u>February</u>	<u>DJF Sum</u>	<u>Natural Gas</u>	<u>Petroleum</u>	<u>Coal</u>	<u>estimated ef</u>
	<u>(Gg C)</u>				<u>(%)</u>			
<u>Airport</u>	<u>8.47</u>	<u>8.74</u>	<u>8.04</u>	<u>25.24</u>	<u>0.0</u>	<u>100.0</u>	<u>0.0</u>	<u>1.05</u>
<u>Commercial</u>	<u>45.30</u>	<u>47.47</u>	<u>35.16</u>	<u>127.92</u>	<u>83.3</u>	<u>16.7</u>	<u>0.0</u>	<u>1.80</u>
<u>Electricity Generation</u>	<u>10.01</u>	<u>6.50</u>	<u>6.84</u>	<u>23.36</u>	<u>100.0</u>	<u>0.0</u>	<u>0.0</u>	<u>1.95</u>
<u>Industry</u>	<u>33.21</u>	<u>33.81</u>	<u>33.21</u>	<u>100.24</u>	<u>46.7</u>	<u>35.1</u>	<u>18.2</u>	<u>1.37</u>
<u>Non-road</u>	<u>8.90</u>	<u>8.59</u>	<u>8.93</u>	<u>26.42</u>	<u>0.0</u>	<u>100.0</u>	<u>0.0</u>	<u>1.05</u>
<u>Onroad</u>	<u>113.50</u>	<u>113.41</u>	<u>108.94</u>	<u>335.85</u>	<u>0.0</u>	<u>100.0</u>	<u>0.0</u>	<u>1.05</u>
<u>Railroad</u>	<u>1.17</u>	<u>1.17</u>	<u>1.06</u>	<u>3.40</u>	<u>0.0</u>	<u>100.0</u>	<u>0.0</u>	<u>1.05</u>
<u>Residential</u>	<u>116.14</u>	<u>125.64</u>	<u>94.48</u>	<u>336.26</u>	<u>100.0</u>	<u>0.0</u>	<u>0.0</u>	<u>1.95</u>
<u>Weighted average ef</u>	<u>1.52</u>	<u>1.53</u>	<u>1.48</u>	<u>1.51</u>				

5 within the SLV are primarily natural gas facilities. Commercial and industrial source emissions were apportioned using the state-wide ratios of carbon emissions across fuel sources for these economic sectors collected by the US Energy Information Administration (EIA, 2015). Commercial sector emissions were assumed to be 83.3% natural gas and 16.7% petroleum, while industrial emissions were assumed to arise from a combustion mixture of 46.8% natural gas, 35.1% petroleum, and 18.1% coal (Table 1). Weighting these economic sectors and fuel sources by their relative emissions amounts yields a Salt Lake County scale estimate of ef of 1.51 for winter, with individual months ranging from 1.48 to 1.53. Based on this analysis, we consider an estimate for ef of 1.5 going forward.

3 Methods

3.1 Estimates of Atmospheric Stratification

10 The SLV experiences periods of enhanced atmospheric stability each winter when cold air pools in the valley under warmer air aloft (Lareau et al., 2013; Whiteman et al., 2014). Atmospheric stratification is present when atmospheric potential temperature increases with height. Nocturnal stratification is common in many settings due to more rapid radiative cooling near the surface than aloft, but the SLV and other mountain topographic basins can experience periods of extended atmospheric stability lasting longer than a diurnal cycle (Lareau et al., 2013; Whiteman et al., 2001, 1999). These periods are commonly referred to as
 15 persistent cold air pools (PCAPs) (Gillies et al., 2010; Green et al., 2015; Malek et al., 2006).

We assess large-scale SLV vertical stability using twice-daily atmospheric sounding data soundings from the Salt Lake City Airport (KSLC, 0Z and 12Z0 and 12 UTC, or 5 and 17 MSTLT). Sounding profiles were obtained from the Integrated Global Radiosonde Archive (IGRA) (Durre and Yin, 2008), and interpolated to 10 m resolution between the surface (~ 1290 m) and

5,000 m. We calculate two metrics of atmospheric stability from the radiosonde data: a bulk valley heat deficit (VHD) and an estimated mixing height. The valley heat deficit-VHD is the energy that must be added between the surface and some height to bring this portion of the atmosphere to the dry adiabatic lapse rate (e.g., $\frac{\partial\theta}{\partial z} = 0.0 \text{ K km}^{-1}$ or $\frac{\partial T}{\partial z} = -9.8 \text{ K km}^{-1}$). Valley heat deficit (VHD)-VHD is calculated following prior studies of winter stability in the SLV (Baasandorj et al., 2017; Whiteman et al., 2014):

$$VHD = c_p \sum_{1290 \text{ m}}^{2200 \text{ m}} \rho(z) [\theta_{2200 \text{ m}} - \theta(z)] \Delta z \quad (1)$$

where c_p is the specific heat capacity at constant pressure for dry air ($1005 \text{ J kg}^{-1} \text{ K}^{-1}$), $\rho(z)$ is the air density as a function of height (kg m^{-3}), $\theta_{2200 \text{ m}}$ and $\theta(z)$ are the potential temperatures at 2200 m above sea level and at height z respectively (K), and Δz is the thickness of each layer (10 m). The upper bound in the VHD calculation (2200 m) is determined by the elevation of the Oquirrh Mountain ridgeline, which forms the western valley boundary. Following Whiteman et al. (2014), we define a PCAP as three or more consecutive soundings with a VHD-VHD $> 4.04 \text{ MJ m}^{-2}$. This VHD threshold of 4.04 MJ m⁻² corresponds to the mean VHD in days where the SLV daily fine particulate matter concentration (PM_{2.5}) exceeds half of the US National Ambient Air Quality Standard for PM_{2.5} (17.5 $\mu\text{g m}^{-3}$) (Whiteman et al., 2014), and has been used in subsequent studies of SLV air quality and atmospheric stability (Baasandorj et al., 2017; Bares et al., 2018). We have retained this convention for intercomparison with prior studies.

~~Mixing heights are estimated from sounding data, with the method used depending~~ Mixing height estimates depend on whether a surface-based temperature inversion (SBI) is present or absent. If the sounding features an SBI surface-based inversion, the mixing height is estimated as the height at the top of the SBI surface-based inversion (Bradley et al., 1993). If there is no SBI surface-based inversion, the mixing height is estimated using a bulk Richardson number method (Vogelezang and Holtslag, 1996; Seidel et al., 2012). The bulk Richardson number, which is a measure of the ratio of buoyancy to shear production of turbulence, is calculated as:

$$Ri(z) = \frac{(g/\theta_{vs})(\theta_v(z) - \theta_{vs})(z - z_s)}{(u(z) - u_s)^2 + (v(z) - v_s)^2 + bu_*^2} \quad (2)$$

where $Ri(z)$ is the bulk Richardson number as a function of height, g is the acceleration due to gravity (9.81 m s^{-2}), θ_v is the virtual potential temperature (K), z is the altitude (m above sea level), u and v are the zonal and meridional wind components (m s^{-1}), and bu_*^2 is the effect of surface friction. A subscript 's' indicates these are surface values. As u_* is not available from radiosonde observations, we assumed frictional effects were negligible (Seidel et al., 2012). This assumption is particularly well justified during stable atmospheric conditions (Vogelezang and Holtslag, 1996), such as during PCAPs. The mixing height was identified as the lowest altitude where $Ri(z)$ was greater than a critical value of 0.25.

3.2 Water Vapor Isotope Data

Water vapor isotope data were collected ~~from using~~ a Picarro L2130-i water vapor isotope analyzer (Santa Clara, CA). Vapor was sampled from the roof of the eight-story ($\sim 35 \text{ m}$ above the ground) William Browning Building (WBB on the University

of Utah campus (UOU, 40.7662°N, 111.8458°W, 1440 m above sea level) ~~on the University of Utah campus~~ through copper (prior to winter 2016/2017) or teflon tubing, using a diaphragm pump operating at $\sim 3 \text{ L min}^{-1}$. Standards were analyzed every 12 hours using the Picarro Standards Delivery Module (SDM), using lab air pumped through a column of anhydrous calcium sulfate (Drierite) as a dry gas source.

5 We calibrated the data using the University of Utah vapor processing scripts, version ~~1.1.1~~ 1.2. Calibration of raw instrument values at $\sim 1 \text{ Hz}$ on the instrument scale to hourly averages on the VSMOW scale proceeds across three stages (~~following Gorski et al., 2015~~): (1) Measured isotope values are corrected for an apparent dependence on cavity humidity, using correction equations developed by operating the ~~SDM standards delivery module~~ at a range of ~~pumping rates~~ (injection rates, corresponding to cavity humidity values of 500-30000 ppm. Instrumental precision is determined in this step, with uncertainties arising both from a decrease in instrument precision with decreasing cavity humidity, and uncertainty in the regression equation to correct for this bias. The humidity correction is determined by a linear regression of the deviation of isotopic composition from the measured isotopic composition at a reference humidity against the inverse of cavity humidity. The reference humidity used is 15,000-25,000 ppm, a range where the instrument response is linear and at which liquid water samples are measured and lab standards are calibrated. Additional details on this correction are provided in a supplement. (2) ~~A background humidity correction is performed to account for incomplete drying of lab air by the drying agent. We assume that 250 of water vapor passes through the drying column and that the water vapor passing through the column has the same isotopic composition as the ambient air measured for the 5 minutes immediately prior to standards measurements (e. g., fractionation by the drying column is negligible).~~ (3) Analyzer measurements are calibrated to the VSMOW-VSLAP scale using two standards of known isotopic composition delivered by the ~~SDM standards delivery module~~, using calibration periods that bracket a series of ambient vapor measurements ~~to correct for analytical drift~~. (3) corrected measurements were aggregated to an hourly time step. Measurement uncertainties are primarily limited by changes in instrument precision with cavity humidity, and 1σ uncertainties range from 0.88‰ for $\delta^{18}\text{O}$, 3.61‰ for $\delta^2\text{H}$, and 7.93‰ for d-excess (assuming error independence) at a humidity of 1000 ppm; to 0.14‰ for $\delta^{18}\text{O}$, 0.53‰ for $\delta^2\text{H}$, and 1.24‰ for d-excess at a humidity of 10000 ppm.

3.3 ~~CO₂~~-CO₂ and ~~meteorological~~ meteorological measurements

25 Meteorological measurements were co-located with water vapor isotope sampling on the roof of the ~~WBB~~ UOU. Temperature, humidity, wind speed, solar radiation, and pressure measurements are all made at 5-min averages (Horel et al., 2002), and were averaged to 1 hour blocks for analysis.

~~CO₂~~-CO₂ measurements were made in two different locations during the study period. Prior to August 2014, ~~CO₂~~-CO₂ measurements were made on the roof of the Aline Skaggs Biology Building (ASB) on the University of Utah campus, ~ 0.25 km south of the ~~WBB~~ ~~CO₂ and H₂O~~ William Browning Building (coded as UOU). CO₂ and H₂O measurements made at ASB were performed using a Li-Cor 7000. Atmospheric air was drawn through a 5 L mixing volume and measured every five minutes. Pressure and ~~H₂O~~-H₂O dilution corrections were applied by the Li-Cor. All measurements were recorded to a Campbell Scientific CR23X.

From August 2014 onwards, CO_2 - CO_2 measurements have been made at the WBB-UOU where they are co-located with meteorological measurements and the water vapor isotope ~~and meteorological measurements~~ described in section 2.2. ~~Atmospheric CO_2~~ 3.2. Atmospheric CO_2 , CH_4 and H_2O - H_2O measurements were performed using a Los Gatos Research Off-Axis Integrated Cavity Output Spectroscopy (Model 907-0011, Los Gatos Research Inc., San Jose, CA). Measurements
 5 were recorded at 0.1 Hz. The effects of water vapor dilution and spectrum broadening (Andrews et al., 2014) were corrected by LGR’s real-time software, and were independently verified through laboratory testing.

At both ASB and WBB-UOU, calibration gases were introduced to the analyzer every three hours using three whole-air, dry, high-pressure reference gas cylinders with known CO_2 - CO_2 concentrations, tertiary to the World Meteorological Organization X2007 CO_2 - CO_2 mole fraction scale (Zhao and Tans, 2006). Concentrations of the calibration gases spanned the expected
 10 range of atmospheric observations. Each standard of known concentration is linearly interpolated between two consecutive calibration periods to represent the drift in the averaged measured standards over time. Ordinary least ~~squared-squares~~ regression is then applied to the interpolated reference values during the atmospheric sampling periods to generate a ~~linear~~-slope and intercept estimates. These are then used to correct all uncalibrated atmospheric observations between calibration periods. Analytical precision is estimated to be ~ 0.1 ppm.

15 Seven months of overlapping data were collected at both ASB and WBB-UOU and analyzed to identify any significant difference in measurement locations. The two locations are highly similar ($\text{CO}_{2,WBB} = 0.98\text{CO}_{2,ASB} + 8.087, r^2 = 0.96$ $\text{CO}_{2,UOU} = 0.98\text{CO}_{2,ASB} + 8.087, r^2 = 0.96$) though pollutants appear to “mix-out” at the end of a PCAP event approximately one hour earlier at ASB relative to WBB-UOU. We do not adjust the ASB time series as the potential time shift is small, and the period of overlapping records is short and does not span a full annual cycle.

20 3.4 Mixing analysis between meteorological humidity and CDV combustion-derived vapor

CDV can be ~~detected by using~~ assessed by considering a two-part isotopic mixing model that treats meteorological or advected vapor and CDV as the end members. We develop a schematic demonstrating the ‘natural’ evolution of d-excess under atmospheric moistening and condensation conditions, as well as through moistening via the addition of CDV. The isotopic composition of an air parcel losing moisture in a Rayleigh condensation process can be modeled as (Gat, 1996):

$$25 \quad \delta = \left[\left(\delta_0 + 1 \right) \left(\frac{q}{q_0} \right)^{\alpha - 1} - 1 \right] \quad (3)$$

where δ is the isotopic composition, q is the specific humidity, and α is the temperature-dependent equilibrium fractionation factor between vapor and the condensate. A subscript zero indicates the initial conditions of a parcel prior to condensation. Humidity is removed from the air parcel through adiabatic cooling starting from the parcel’s initial dew point temperature and cooling in 0.5 K intervals to 243 K; progressive cooling is used to account for changes in α with temperature. $\delta^{18}\text{O}$
 30 and $\delta^2\text{H}$ are modeled separately and then combined to estimate the evolution of d-excess throughout condensation. We used fractionation factors for vapor over liquid for temperatures above 273 K (Horita and Wesolowski, 1994) and for vapor over ice for temperatures below 253 K (Majoube, 1970; Merlivat and Nief, 1967). We interpolated α values between 273 K and 253 K to account for mixed-phase processes between these temperatures. As the heavy isotopes of both oxygen and hydrogen are

progressively removed through condensation, d-excess increases as humidity is decreased, approaching a limit of 7000‰ if all ^2H and ^{18}O were removed (Bony et al., 2008).

We also modeled the isotopic evolution of d-excess in an air parcel in the absence of CDV experiencing mixing between the moist and dry end members of the Rayleigh distillation curve. D-excess is modeled throughout this humidity range as a mass-weighted mixing model average of the d-excess values of both end members:

$$d_{\text{mix}} = \frac{d_{\text{dry}}q_{\text{dry}} + d_{\text{moist}}q_{\text{moist}}}{q_{\text{dry}} + q_{\text{moist}}} \quad (4)$$

Likewise, moistening of the lower troposphere by CDV can be modeled as a mixing process between CDV and the background “natural” water vapor:

$$d_{\text{mix}} = \frac{d_{\text{CDV}}q_{\text{CDV}} + d_{\text{bg}}q_{\text{bg}}}{q_{\text{mix}}} \quad (5)$$

where subscripts CDV, bg, and mix refer to properties of CDV, the atmospheric moisture in the absence of CDV, and values of the mixed parcel, respectively. Gorski et al. (2015) assumed a mean value of -225‰ for d_{CDV} based on a few direct measurements of CDV. Adopting this value, we construct a model framework to explain changes in d-excess relative to humidity expected from natural condensation and mixing pathways as well as the addition of moisture via CDV (Fig. 1), but also revisit this assumption based on further analysis of our data (below). Drying the atmosphere by mixing in a dry air mass in the absence of CDV or by Rayleigh condensation increases the d-excess of ambient vapor, whereas atmospheric moistening occurring due to mixing with a moist air mass can decrease the d-excess of ambient vapor. The response of d-excess due to these natural processes is non-linear with respect to changes in humidity, and very similar between condensation and mixing of “natural” air masses (Fig. 1). In contrast, small mass additions of CDV (up to 500 ppm) produce a strong, quasi-linear decrease in d_{mix} with increasing q_{CDV} (Fig. 1). Assuming a representative ef value of 1.5 (section 2), 100 or 500 ppm of CDV correspond to CO_2 increases of 66.7 or 333.3 ppm, respectively. Deviation from the “natural” air mass mixing line is greatest at low q_{bg} for a given q_{CDV} , as CDV comprises a larger fraction of q_{mix} .

Finally, recasting these mixing-model equations following Miller and Tans (2003) the Miller-Tans (2003) formulation of the Keeling (1958; 1961) mixing model, we can estimate d_{CDV} using a Keeling-style approach (1958; 1961). In this framework, the product of observed d and q (e.g., d_{obs} and q_{obs}) is proportional to q_{CDV} :

$$d_{\text{obs}}q_{\text{obs}} = d_{\text{CDV}}q_{\text{CDV}} + d_{\text{bg}}q_{\text{bg}} \quad (6)$$

If we assume that q_{CDV} is linearly related to the increase in CO_2 above background concentrations, d_{CDV} can be estimated as the slope of a linear regression between observed d and observed CO_2 and observed $d_{\text{obs}}q_{\text{obs}}$ and observed CO_2 concentrations:

$$d_{\text{obs}}q_{\text{obs}} = d_{\text{CDV}}(ef)[\text{CO}_2 - \min(\text{CO}_2)] + d_{\text{bg}}q_{\text{bg}} \quad (7)$$

where ef is the emissions factor, which is the stoichiometric ratio of H_2O to CO_2 in combustion products, and $[\text{CO}_2 - \min(\text{CO}_2)]$ represents the amount of excess CO_2 in the atmosphere above the background value. The ef parameter depends on the molar ratios of hydrogen to carbon in the fuel source; we estimate an fuel-source-weighted

SLV-scale ef value for winter of 1.5, but note that ef values for hydrocarbon fuels can vary from $< 0.5 - 2$. We define the background CO_2 value, $\min(CO_2)$, to be the seasonal minimum value observed at the WBB-UOU or the ASB. Observations of urban $\delta^{13}C-CO_2$ and atmospheric modeling of the SLV indicate that wintertime increases in CO_2 above background concentrations are driven by anthropogenic emissions, and that the contribution from local respiration to urban CO_2 enhancement is likely negligible (Pataki et al., 2003, 2005, 2007; Strong et al., 2011). We apply two linear mixed models where the intercept-PCAP-to-PCAP event-scale variability is treated as a random factor-effect to estimate d_{CDV} : in the first, year-to-year variability is treated as a random effect the slope is assumed to be constant across all PCAP events but the intercept is allowed to vary, while in the second, PCAP-to-PCAP event-scale variability is treated as a random effect both the slope and intercept are allowed to vary across PCAP events. These models are constructed to find the best-fit slope, and therefore the best-fit estimate of d_{CDV} , across all PCAP events. As a result, they implicitly assume that changes in d_{CDV} through time are small compared to changes in $d_{bg}q_{bg}$, or that changes in the emissions profile and components of the SLV are small compared to environmental variability in humidity and d-excess. We consider only the second model in our results as we find it has more support than the first model, with this selection determined based on lower AIC and BIC scores for the second model.

Finally, the fraction of urban humidity comprised of CDV can be estimated by solving equation 6 for q_{CDV}/q_{obs} using the constraint that $q_{obs} = q_{CDV} + q_{bg}$:

$$\frac{q_{CDV}}{q_{obs}} = \frac{d_{obs} - d_{bg}}{d_{CDV} - d_{bg}} \quad (8)$$

Using this equation, we estimate a maximum contribution of CDV to boundary layer humidity for each PCAP where water isotope data are available using the minimum d_{obs} value from each PCAP. We assume a constant value of d_{CDV} , determined from the slope of the linear mixed model described above. Two estimates of d_{bg} were made for each PCAP based on the assumptions that d_{bg} reflects: (a) the mean observed d value for the 12 hours prior to the initiation of the PCAP, or (b) the mean d value for the 12 hour period where the 12 hour moving average CO_2 concentration falls below 415 ppm. For (b), if the 12 hour average CO_2 concentration fails to fall below 415 ppm between two PCAPs, d_{bg} is estimated from the minimum CO_2 value between these PCAP events.

4 Results

We observed 26 PCAP events across four winters, with seven, four, seven, and eight occurring during DJF 13/14, 14/15, 15/16, and 16/17, respectively (Fig. 2). VHD exceeded $4.04 MJ m^{-2}$ for a 30%, 18%, 27%, and 25% of the observed KSLC soundings during each winter. Variability of 1 to $2 MJ m^{-2}$ between consecutive soundings is common, and results from the diurnal cycle of surface heating during the day and radiative cooling at night (Whiteman et al., 2014). Calculated mixing heights ranged from the surface ($1290-0 m$) to $4680-AGL$ to $3390 m AGL$, with a median value of $1560-270 m AGL$. The mean mixing height and its variance are low in December and January, though both increase in February as solar radiation increases and more energy is available to grow the daytime convective boundary layer. CO_2

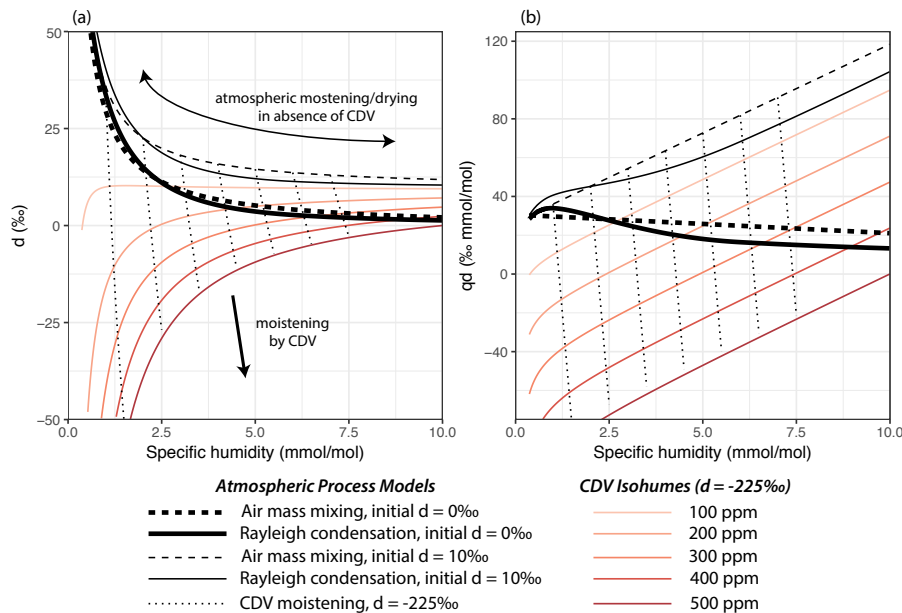


Figure 1. Schematic of expected changes in the d-excess of atmospheric vapor with changes in humidity associated with atmospheric moistening and drying in the absence of CDV due to Rayleigh distillation (solid black lines) or air mass mixing (dashed black lines) or the addition of CDV (dotted black lines). Models for Rayleigh distillation and air mass mixing are shown for two initial d-excess values of the moist end member: 0‰ (thin-thick lines) and 10‰ (thick-thin lines). Panel (a) shows this relationship of d (‰) vs specific humidity, q (mmol mol^{-1}), where mixing processes trace hyperbolic pathways, and panel (b) shows the same models but with axes of qd (‰ mmol mol^{-1}) against q (mmol mol^{-1}), where mixing processes are linear. Finally, lines across a yellow-to-red-red gradient are drawn to show the impact of fixed amounts of CDV addition ranging from 100 ppm (yellowlight) to 500 ppm (reddark) as a function of specific humidity.

CO₂ concentrations show close inverse associations with measured d-excess values across diurnal to synoptic timescales (Fig. 3). CO₂ Paired d-excess and CO₂ measurements are available for 76.8% of the period of record, including for 22 of the 26 PCAP events. CO₂ concentrations and d-excess values were inversely cross-correlated for all four winter periods ($r = -0.555, -0.555, -0.497, \text{ and } -0.665$ $r = -0.589, -0.547, -0.428, \text{ and } -0.527$ for each consecutive winter). The maximum cross-correlation was observed with zero lag in DJF 14/15 and 16/17, whereas d-excess lagged CO₂-CO₂ by 1 hour in DJF 13/14 and 15/16. For each winter season, minimum/maximum hourly CO₂-CO₂ concentrations were 397/637 ppm, 400/581 ppm, 404/598 ppm, 406/653 ppm, whereas minimum/maximum hourly d-excess values were -23.8/33.9‰, -5.2/33.4‰, -3.3/17.6-26.4/24.5‰, -10.5/19.4‰, -8.0/12.9‰, and -17.6/16.1-26.8/14.3‰.

During each PCAP event, CO₂-CO₂ was elevated relative to its background value. For most PCAP events, d-excess decreased commensurately with the increase in CO₂-CO₂; however, several exceptions were observed. For example, PCAPs in February 2016 and 2017 showed diurnal cyclicity in d-excess and CO₂, but mean concentrations through the event remained fairly stable CO₂ during the event, but these periods often exhibited a multiday period of CO₂ increase and d-excess decrease prior

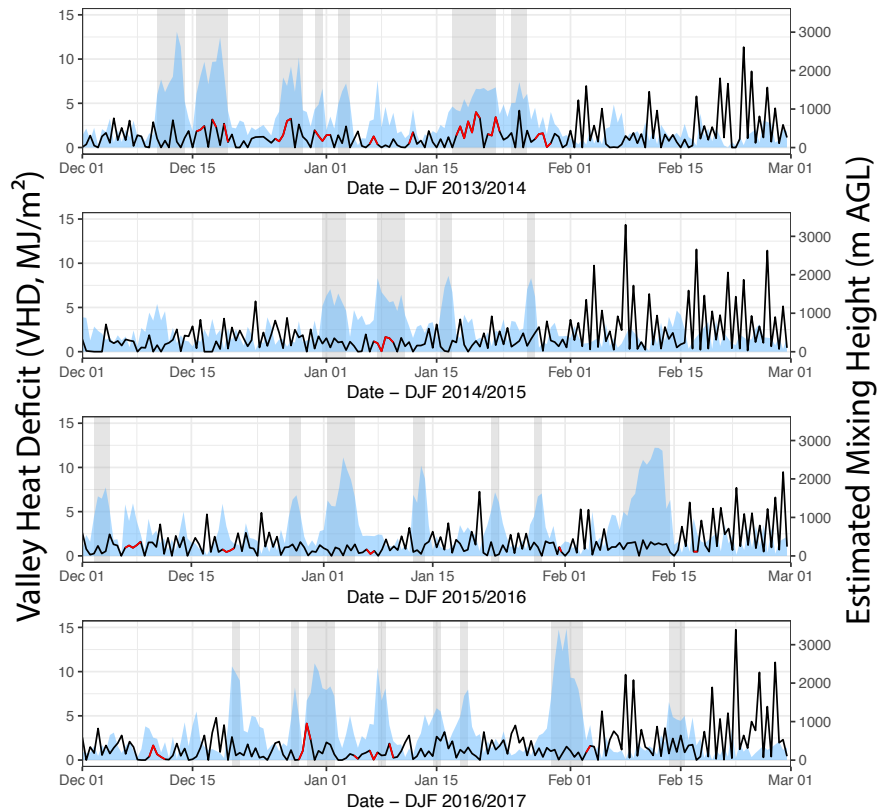


Figure 2. Valley heat deficit (MJ m^{-2} , blue polygon) and mixing height (m, black indicates Richardson mixing height; red indicates surface-based inversion top) by season. Seven, four, seven, and eight PCAP events are identified for DJF 13/14, 14/15, 15/16, and 16/17, and are denoted by light gray shading.

to atmospheric stability reaching the VHD threshold for a PCAP. In these events, the bulk of the d-excess decrease occurs prior to the onset of the PCAP as defined by the VHD metric, and d-excess exhibits strong diurnal variability but with a small longer-term trend during the event before increasing when the PCAP ends. Additionally, elevated CO_2 - CO_2 and depressed d-excess values were frequently observed in the absence of PCAPs (e.g., mid-December 2014 and 2016); these cases are associated with low mixing heights, but not necessarily high ~~VHD values~~ VHD values, or of moderate VHD values that fell short of the VHD-based definition of a PCAP.

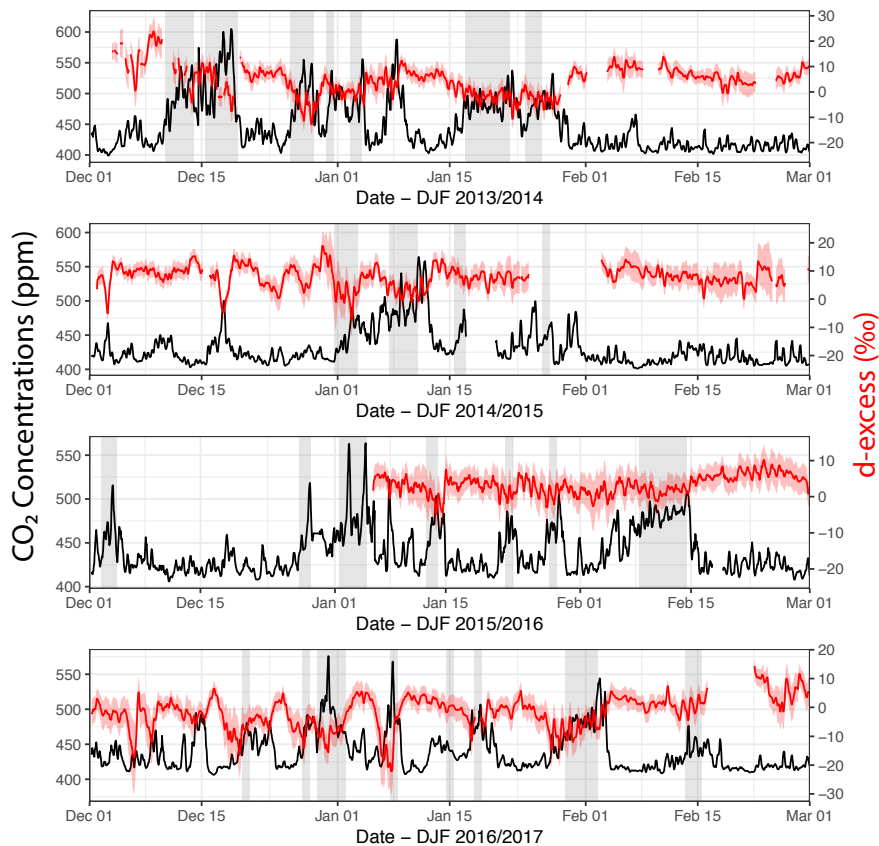


Figure 3. Six hour running-mean CO_2 -CO₂ concentrations (ppm, black line) and water vapor d-excess (‰ VSMOW, red line, 2σ uncertainty shown in red shading) measured at the WBB-UOU for DJF 2013-2017. Persistent cold air pool events are denoted by gray rectangles. When the lower atmosphere is stable, CO_2 -CO₂ builds up in the boundary layer and d-excess tends to decrease.

4.1 Relationship between $\delta^{13}\text{C}_{\text{CO}_2}$ - CO_2 and d-excess and estimating d-excess of CDV

Clear distinctions emerged in the distributions of $\delta^{13}\text{C}_{\text{CO}_2}$ - CO_2 and d-excess during PCAP events compared to more well-mixed periods (Fig. ??). Non-PCAP periods are typically defined by lower $\delta^{13}\text{C}_{\text{CO}_2}$ - CO_2 values, usually below 450 ppm, and a broad range of d-excess values averaging around $\sim 10\text{‰}$ and spanning $\sim 0 - 30 \text{‰}$ (Fig. 3). D-excess variability during non-PCAP periods is likely controlled by natural moistening and dehydration processes, including air mass mixing, Rayleigh-style condensation and evaporative inputs from the Great Salt Lake. In contrast, a strong linear relationship between $\delta^{13}\text{C}_{\text{CO}_2}$ - CO_2 and d-excess is observed during PCAP periods, with d-excess values decreasing proportionally with increasing $\delta^{13}\text{C}_{\text{CO}_2}$ - CO_2 . At the highest $\delta^{13}\text{C}_{\text{CO}_2}$ - CO_2 concentrations, d-excess can be $>10\text{‰}$ lower than when $\delta^{13}\text{C}_{\text{CO}_2}$ - CO_2 is at background levels outside of PCAP events.

Distributions of CO_2 and d-excess for DJF 13/14 (first row), 14/15 (second row), 15/16 (third row) and 16/17 (fourth row). Conditions during PCAP events are shown in blue contours and non-PCAP periods are shown in red contours. Non-PCAP periods are marked by lower CO_2 concentrations (<450) and a broad range of positive d-excess values, PCAP periods show a strong linear relationship, with decreasing d-excess values associated with increasing CO_2 concentrations. These relationships between “natural” moistening and drying of the boundary layer and moistening by CDV become apparent from the relationship between d-excess and humidity (Fig. 4). Changes in d-excess and q from atmospheric moistening and drying processes in the absence of CDV are expected to follow a hyperbolic or near-hyperbolic relationship, and trend toward increasing d-excess values at low humidities (Fig. 1). In contrast, addition of CDV to the atmosphere will promote strong negative deviations from this $q-d$ relationship that are proportional to amount of CDV, and are essentially linear over likely ranges of q_{CDV} . These patterns are observed in our measurements, where d-excess values are high and trend upward for low humidities at low CO_2 concentrations, and show linear patterns of decrease with increasing CO_2 . We observe increasing qd values with increasing q at low CO_2 concentrations, but decreasing qd values with increasing CO_2 (Fig. 4). Strong positive d-excess excursions are observed during the first two winters, and are associated with dry, cold conditions following the passage of a strong cold front. No equivalent excursions are observed during the last two winters, perhaps due to a similar magnitude cold front event not occurring during the observed portions of those winters. Negative excursions are observed during PCAP events or when $\delta^{13}\text{C}_{\text{CO}_2}$ is elevated, and can be seen across a range of humidity values.

We leverage the observed, coupled variability in d-excess and $\delta^{13}\text{C}_{\text{CO}_2}$ - CO_2 during periods of enhanced $\delta^{13}\text{C}_{\text{CO}_2}$ - CO_2 to test previous theoretical estimates and limited source-direct measurements of d_{CDV} using a Keeling-style approach (1958; 1961). Recall that d_{CDV} can be estimated as the slope of a regression between $q_{\text{obs}}/d_{\text{obs}}$ and q_{CDV} . We approximate q_{CDV} by multiplying the enrichment of CO_2 above its background value by an emissions factor, ef , which represents the stoichiometric ratio of $\text{H}_2\text{O}:\text{CO}_2$ in combustion products (Gorski et al., 2015). The best-fit slope of a linear mixed model allowing for random variation in the both the slope and intercept between PCAP events yields an estimate of d_{CDV} of $-308 \pm 12 - 179 \pm 17\text{‰}$ for $ef = 1.0$ and $-154 \pm 6\text{‰}$ for $ef = 2.0$ $ef = 1.5$ (Fig. 5). A similar model, allowing the intercept to vary by season instead of by event, yields comparable estimates of This estimate of d_{CDV} of -250 ± 15 is consistent with the upper limit of theoretical estimates and pilot measurements from Gorski et al. (2015), and could be further validated by a comprehensive survey of fuels

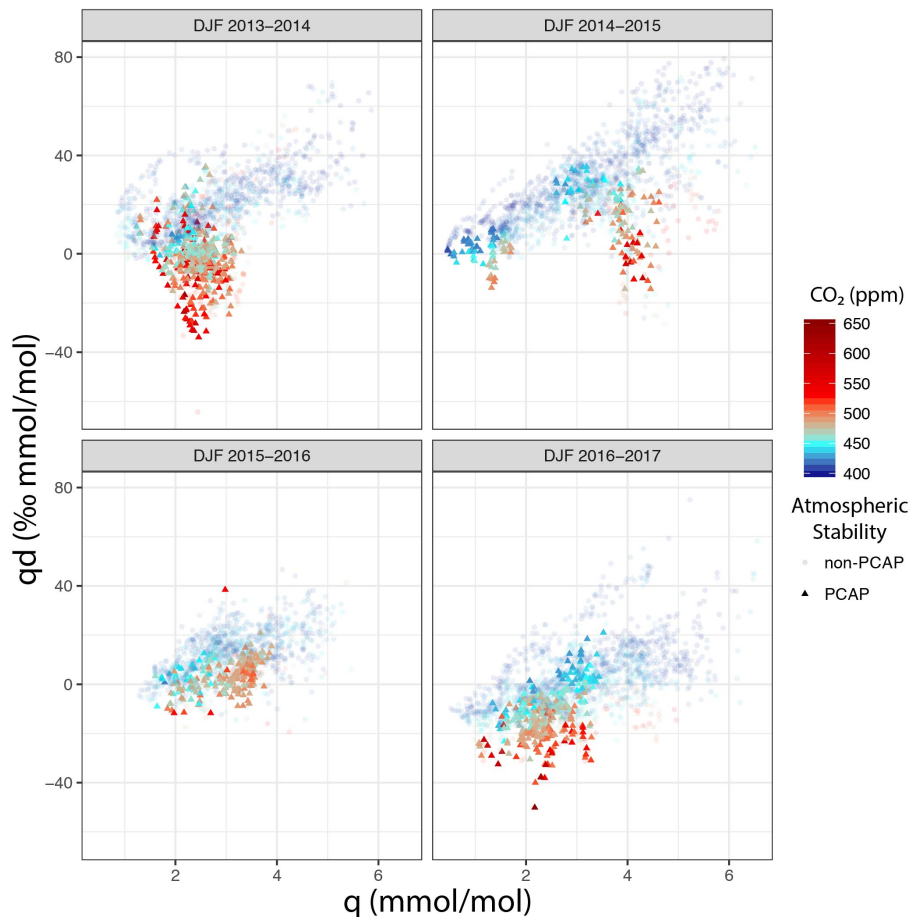


Figure 4. Relationship of the product of specific humidity and d-excess, qd ($\% \text{ mmol mol}^{-1}$), against specific humidity q (mmol mol^{-1}). Points are colored by CO_2 - CO_2 concentration (ppm) at the time of measurement, with the shape and shapes correspond opacity corresponding to if whether the data point was collected during a PCAP event (opaque triangles) or outside of a PCAP event (semitransparent circles). Moistening and drying by condensation and mixing of “natural” air masses occurs along a line with positive slope, while moistening by CDV occurs along a line with negative slope.

in the SLV. Based on this regression, d-excess decreases by $0.18 \pm 0.02\%$ for $ef=1.0$ every ppm increase in CO_2 , though this rate of change will vary slightly with background q (Fig. 1). Instrumental precision (1σ) for d-excess is estimated to be 2.4% at the mean DJF humidity value of 4 mmol mol^{-1} , implying that enrichments of $\sim 40 \text{ ppm}$ CDV can be detected at the 2σ level. This estimated detection limit will likely decrease as instrument precision and calibration routines are improved, and may change in other locations with different fuel use patterns and ef values. For individual PCAPs, the slope of the regression and the strength of the correlation between $q_{\text{obs}}d_{\text{obs}}$ and $-125 \pm 7\text{CO}_2$ excess are more variable, with slopes ranging from $-25 \pm 43\%$ for $ef=2.0$. The former model is likely to be more robust as it better accounts for meteorological variability between events. The range of to $-379 \pm 63\%$ and coefficients of determination ranging from 0.77 to 0.001 (Table 2). The wide

range of slopes and coefficients of determination observed hints at a complex relationship between urban humidity, CO_2 , and CDV that varies with the nature of each period of high atmospheric stability. For example, fuel mixtures and heating demands may change with temperature, inversions based on the valley floor may trap most pollutants below the UOU observation site, and other sources and processes such as advection or evaporation over the Great Salt Lake may also contribute water vapor to the boundary layer and alter the relationship between $q_{\text{obs}}d_{\text{obs}}$ and CO_2 excess. Expanding observations beyond a single site (UOU) may help distinguish these possibilities.

Using this estimate for d_{CDV} estimates from these observations are consistent with theoretical models from (Gorski et al., 2015), though uncertainty in a representative value of ϵ_f across time and from the mixture of fuel sources and combustion systems in the SLV prohibits a precise determination of d_{CDV} . of $-179 \pm 17\%$, we estimate the maximum fraction of CDV for each PCAP event using equation 8 and estimates of d_{bg} from both the 12 hour period prior to PCAP initiation, or the last 12 hour period with a CO_2 minimum. When the former assumption is used for d_{bg} , estimates of the CDV fraction average 5.0% across all PCAP events, and range from $-2.1 \pm 2.3\%$ to $13.9 \pm 1.9\%$, while when the latter assumption for d_{bg} is used, the mean CDV fraction rises to 7.2% and ranges from $2.2 \pm 2.1\%$ to $16.7 \pm 3.2\%$ (Table 3). Negative CDV fraction estimates occur when the estimated d_{bg} is less than the minimum value of d_{obs} , and are only observed when the 12 hour period immediately preceding the initiation of the PCAP is used to estimate d_{bg} . CO_2 concentrations can build up whenever the atmosphere is stable, even if atmospheric stability has not yet met the PCAP threshold used here. Therefore, this pattern highlights the importance and challenge of accurately estimating d_{bg} for this humidity apportionment method to yield accurate estimates of $q_{\text{CDV}}/q_{\text{obs}}$.

4.2 Case studies

4.2.1 December 2228, 2014-January 14, 2015

Two distinct PCAP events were observed between December 2228, 2014 and January 14, 2015 (Fig. 6). Conditions at the beginning of this period were humid (~ 8) and warm ($\sim 5^\circ$), and both values fell rapidly to ~ 1.75 . The period prior to the first PCAP is marked by a cold front passage around December 30, 2014 12 UTC, where there are strong decreases in temperature and humidity (Fig. 6b) and -12° ab), elevated wind speeds (Fig. 6c) thorough December 30, 2014 12Z as a cold front entered the region, a CO_2 minimum (Fig. 6f) ahead of the first PCAP event. During this period of atmospheric drying, d), and an increase in d-excess rose from 10 to $\sim 18\%$ to $>30\%$ (Fig. 6a), consistent with dehydration through either a condensation process or entrainment of a dry air mass.) that is generally consistent with natural removal of water from the atmosphere (Fig. 6f). After onset of the PCAP, however, d-excess dropped rapidly as CO_2 - CO_2 and CDV began to build in the valley. By January 2, CO_2 - CO_2 had risen to 480-490 ppm and d-excess had fallen to $\sim 5-7.4\%$, an increase of ~ 60 ppm and a decrease of 25% respectively (Fig. 6a, d, e). Atmospheric d-excess through this period closely followed model expectations of moistening via CDV (Fig. 6a, f). After the end of the first PCAP event, specific humidity and temperature rose daily until the start of the second PCAP on January 7 12Z, 12 UTC (Fig. 6ab). During this period in between PCAP events, CO_2 - CO_2 remained elevated, and exhibited diurnal variability of 20-40 ppm (Fig. 6e). Changes in d), but d-excess were consistent with diurnal cycles in d-excess driven by CDV inputs superimposed on a longer-term moistening trend remained more consistent

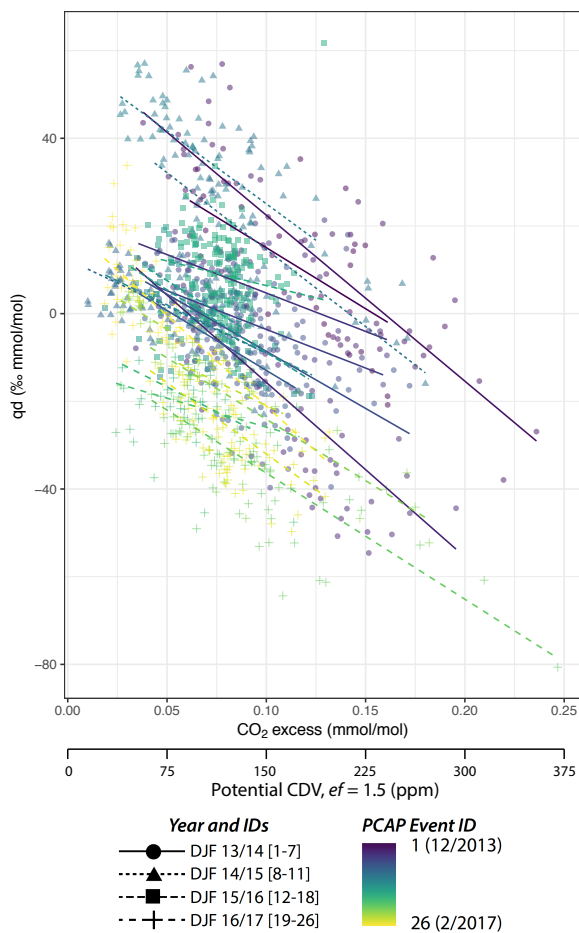


Figure 5. Keeling-style Miller-Tans style plots of q_d ($\% \text{ mmol mol}^{-1}$) versus CO_2 CO_2 -excess (the difference between the observed CO_2 and the seasonal minimum CO_2) by year during PCAP events. The estimated d-excess of CDV, assuming CDV is the dominant flux of water into the boundary layer during PCAP events, is the slope of the best fit line. The best-fit linear mixed-model that keeps the slope identical across-years but allows for variability in the intercept is shown for each year.

(Fig. 6d). Despite the VHD falling below the PCAP threshold in between PCAP events (Fig. 2), the lower atmosphere did not become well-mixed. Airport soundings indicated an elevated inversion atop a saturated cloud layer remained during this period, which decreased surface solar heating (Fig. 6e) while wind speeds remained low (Fig. 6f). As a result, CO_2 concentrations did not return to background values (Fig. 6d-e). Together, the pattern of d-excess and CO_2 change across between the two PCAP events is consistent with “natural” moistening of the boundary layer paired with an incomplete mix-out of CDV and CO_2 . The second PCAP event, spanning January 7 12Z-12 UTC until January 11 00Z-00 UTC, was marked by prominent diurnal cycles in humidity, temperature, and CO_2 - CO_2 (Fig. 6a-ea,b,d). Strong diurnal cyclicality was also observed in d-excess (Fig. 6d). Humidity additions were most likely a mixture of CDV and evaporation from the Great Salt Lake or sublimation of snowfall.

Table 2. Miller-Tans regression parameters for each PCAP event

<u>Start of PCAP</u>	<u>End of PCAP</u>	<u>Regression Slope ($ef = 1.5$)</u>	<u>Regression R^2</u>
<u>10 Dec 2013 1200</u>	<u>14 Dec 2013 0000</u>	<u>-190 ± 46</u>	<u>0.33</u>
<u>15 Dec 2013 1200</u>	<u>19 Dec 2013 1200</u>	<u>-260 ± 21</u>	<u>0.77</u>
<u>26 Dec 2013 0000</u>	<u>29 Dec 2013 0000</u>	<u>-275 ± 27</u>	<u>0.62</u>
<u>30 Dec 2013 1200</u>	<u>31 Dec 2013 1200</u>	<u>-89 ± 45</u>	<u>0.17</u>
<u>02 Jan 2014 1200</u>	<u>04 Jan 2014 0000</u>	<u>-101 ± 41</u>	<u>0.13</u>
<u>17 Jan 2014 0000</u>	<u>22 Jan 2014 1200</u>	<u>-173 ± 25</u>	<u>0.30</u>
<u>24 Jan 2014 1200</u>	<u>26 Jan 2014 1200</u>	<u>-185 ± 35</u>	<u>0.34</u>
<u>31 Dec 2014 1200</u>	<u>03 Jan 2015 1200</u>	<u>-134 ± 22</u>	<u>0.42</u>
<u>07 Jan 2015 1200</u>	<u>11 Jan 2015 0000</u>	<u>-241 ± 39</u>	<u>0.34</u>
<u>15 Jan 2015 1200</u>	<u>17 Jan 2015 0000</u>	<u>-228 ± 46</u>	<u>0.59</u>
<u>12 Jan 2016 1200</u>	<u>14 Jan 2016 0000</u>	<u>-128 ± 38</u>	<u>0.25</u>
<u>22 Jan 2016 1200</u>	<u>23 Jan 2016 1200</u>	<u>-199 ± 39</u>	<u>0.55</u>
<u>28 Jan 2016 0000</u>	<u>29 Jan 2016 0000</u>	<u>-206 ± 99</u>	<u>0.15</u>
<u>08 Feb 2016 1200</u>	<u>14 Feb 2016 1200</u>	<u>-25 ± 43</u>	<u>0.001</u>
<u>20 Dec 2016 0000</u>	<u>21 Dec 2016 0000</u>	<u>-130 ± 54</u>	<u>0.06</u>
<u>27 Dec 2016 1200</u>	<u>28 Dec 2016 1200</u>	<u>-45 ± 54</u>	<u>0.005</u>
<u>29 Dec 2016 1200</u>	<u>02 Jan 2017 0000</u>	<u>-193 ± 18</u>	<u>0.52</u>
<u>07 Jan 2017 1200</u>	<u>08 Jan 2017 1200</u>	<u>-189 ± 39</u>	<u>0.34</u>
<u>14 Jan 2017 1200</u>	<u>15 Jan 2017 1200</u>	<u>-379 ± 63</u>	<u>0.64</u>
<u>18 Jan 2017 0000</u>	<u>19 Jan 2017 0000</u>	<u>-41 ± 30</u>	<u>0.44</u>
<u>29 Jan 2017 1200</u>	<u>02 Feb 2017 1200</u>	<u>-232 ± 32</u>	<u>0.08</u>
<u>13 Feb 2017 1200</u>	<u>15 Feb 2017 1200</u>	<u>-328 ± 40</u>	<u>0.62</u>

The last day of the PCAP exhibited a strong decrease in solar irradiance (Fig. 6c), which likely indicated cloud development at the base of an elevated inversion, a feature typical of extended PCAP events (Baasandorj et al., 2017; Whiteman et al., 2014). CO_2 concentrations reached their maximum at the end of the PCAP event, and decreased slowly during the first diurnal cycle after the breakup of the PCAP, before mixing out nearly completely on January 12. Deuterium excess D-excess values followed changes in CO_2 , remaining low but increasing with decreasing CO_2 during the first diurnal cycle, before rapidly increasing as CO_2 decreased at the end of the observation period (Fig. 6de). The spike in CO_2 at the termination of the PCAP is likely due to the WBBUOU's location on a topographic bench; strong stability during the PCAP may have kept the most polluted air below the WBBUOU, which then was transported to higher altitudes as the PCAP ended.

Table 3. Estimates of CDV humidity fraction

<u>Start of PCAP</u>	<u>End of PCAP</u>	<u>Min d_{obs}</u>	<u>Estimated d_{nat}</u> (12h mean before PCAP)	<u>Estimated d_{nat}</u> (last 12h period with CO ₂ < 415 ppm)	<u>q_{CDV}/q_{obs}</u> (12h mean before PCAP)	<u>q_{CDV}/q_{obs}</u> (last 12h period with CO ₂ < 415 ppm)
<u>10 Dec 2013 1200</u>	<u>14 Dec 2013 0000</u>	<u>-7.0 ± 2.3</u>	<u>20.8 ± 0.5</u>	<u>20.3 ± 1.7</u>	<u>13.9 ± 1.9</u>	<u>13.7 ± 2.4</u>
<u>15 Dec 2013 1200</u>	<u>19 Dec 2013 1200</u>	<u>-10.9 ± 2.0</u>	<u>7.7 ± 1.2</u>	<u>7.5 ± 1.4^c</u>	<u>10.0 ± 2.0</u>	<u>9.9 ± 2.1</u>
<u>26 Dec 2013 0000</u>	<u>29 Dec 2013 0000</u>	<u>-13.8 ± 1.9</u>	<u>2.6 ± 1.5</u>	<u>7.0 ± 1.4</u>	<u>9.0 ± 2.1</u>	<u>11.2 ± 2.1</u>
<u>30 Dec 2013 1200</u>	<u>31 Dec 2013 1200</u>	<u>-4.1 ± 1.8</u>	<u>4.9 ± 1.4</u>	<u>0.6 ± 1.4^b</u>	<u>4.9 ± 1.8</u>	<u>2.6 ± 1.8</u>
<u>02 Jan 2014 1200</u>	<u>04 Jan 2014 0000</u>	<u>-8.1 ± 1.6</u>	<u>0.3 ± 1.3</u>	<u>0.7 ± 1.3^c</u>	<u>4.7 ± 1.7</u>	<u>4.9 ± 1.7</u>
<u>17 Jan 2014 0000</u>	<u>22 Jan 2014 1200</u>	<u>-9.6 ± 1.8</u>	<u>-1.0 ± 1.4</u>	<u>8.3 ± 1.3</u>	<u>4.8 ± 1.9</u>	<u>9.6 ± 1.9</u>
<u>24 Jan 2014 1200</u>	<u>26 Jan 2014 1200</u>	<u>-7.8 ± 2.2</u>	<u>1.3 ± 1.4</u>	<u>1.8 ± 1.4^b</u>	<u>5.0 ± 2.1</u>	<u>5.3 ± 2.1</u>
<u>31 Dec 2014 1200</u>	<u>03 Jan 2015 1200</u>	<u>-10.5 ± 2.6</u>	<u>9.7 ± 2.2^d</u>	<u>9.7 ± 2.2^d</u>	<u>10.7 ± 2.8</u>	<u>10.7 ± 2.8</u>
<u>07 Jan 2015 1200</u>	<u>11 Jan 2015 0000</u>	<u>-3.6 ± 1.3</u>	<u>3.5 ± 1.2</u>	<u>12.6 ± 1.3^b</u>	<u>3.9 ± 1.4</u>	<u>8.5 ± 1.6</u>
<u>15 Jan 2015 1200</u>	<u>17 Jan 2015 0000</u>	<u>2.2 ± 2.0</u>	<u>10.8 ± 1.4</u>	<u>8.4 ± 1.4^b</u>	<u>4.5 ± 1.8</u>	<u>3.3 ± 1.8</u>
<u>12 Jan 2016 1200</u>	<u>14 Jan 2016 0000</u>	<u>-5.9 ± 2.2</u>	<u>2.6 ± 1.7</u>	<u>3.2 ± 1.7</u>	<u>4.7 ± 2.2</u>	<u>5.0 ± 2.2</u>
<u>22 Jan 2016 1200</u>	<u>23 Jan 2016 1200</u>	<u>-4.3 ± 1.9</u>	<u>2.0 ± 3.6</u>	<u>3.6 ± 1.6</u>	<u>3.5 ± 2.0</u>	<u>4.3 ± 2.0</u>
<u>28 Jan 2016 0000</u>	<u>29 Jan 2016 0000</u>	<u>-3.4 ± 2.1</u>	<u>-1.1 ± 1.5</u>	<u>2.0 ± 1.6^b</u>	<u>1.3 ± 2.0</u>	<u>3.0 ± 2.1</u>
<u>08 Feb 2016 1200</u>	<u>14 Feb 2016 1200</u>	<u>-2.7 ± 1.9</u>	<u>2.2 ± 1.4</u>	<u>2.6 ± 1.3</u>	<u>2.7 ± 1.8</u>	<u>2.9 ± 1.8</u>
<u>20 Dec 2016 0000</u>	<u>21 Dec 2016 0000</u>	<u>-9.8 ± 2.3</u>	<u>-12.9 ± 2.0</u>	<u>2.5 ± 1.3</u>	<u>-1.9 ± 2.8</u>	<u>6.8 ± 2.3</u>
<u>27 Dec 2016 1200</u>	<u>28 Dec 2016 1200</u>	<u>-17.0 ± 2.9</u>	<u>-8.4 ± 1.7</u>	<u>-3.5 ± 1.4</u>	<u>5.0 ± 2.8</u>	<u>7.7 ± 2.6</u>
<u>29 Dec 2016 1200</u>	<u>02 Jan 2017 0000</u>	<u>-23.1 ± 2.3</u>	<u>-7.6 ± 1.5</u>	<u>-6.0 ± 1.4^c</u>	<u>9.0 ± 2.4</u>	<u>9.9 ± 2.4</u>
<u>07 Jan 2017 1200</u>	<u>08 Jan 2017 1200</u>	<u>-25.9 ± 3.9</u>	<u>-18.0 ± 2.0</u>	<u>4.7 ± 1.2</u>	<u>4.9 ± 3.7</u>	<u>16.7 ± 3.2</u>
<u>14 Jan 2017 1200</u>	<u>15 Jan 2017 1200</u>	<u>-2.4 ± 1.9</u>	<u>0.6 ± 1.4</u>	<u>4.5 ± 1.2</u>	<u>1.7 ± 1.8</u>	<u>3.8 ± 1.7</u>
<u>18 Jan 2017 0000</u>	<u>19 Jan 2017 0000</u>	<u>-4.9 ± 2.3</u>	<u>-8.4 ± 1.6</u>	<u>-0.9 ± 1.4^b</u>	<u>-2.1 ± 2.3</u>	<u>2.2 ± 2.1</u>
<u>29 Jan 2017 1200</u>	<u>02 Feb 2017 1200</u>	<u>-14.7 ± 3.1</u>	<u>-7.8 ± 1.7</u>	<u>3.8 ± 1.3</u>	<u>4.0 ± 2.8</u>	<u>10.1 ± 2.6</u>
<u>13 Feb 2017 1200</u>	<u>15 Feb 2017 1200</u>	<u>-9.4 ± 2.1</u>	<u>1.0 ± 1.4</u>	<u>1.2 ± 1.2</u>	<u>5.8 ± 2.0</u>	<u>5.9 ± 1.9</u>

a: d_{bg} estimated with $415 \text{ ppm} < \text{CO}_2 < 425 \text{ ppm}$

b: d_{bg} estimated with $425 \text{ ppm} < \text{CO}_2 < 450 \text{ ppm}$

c: d_{bg} estimated with $450 \text{ ppm} < \text{CO}_2 < 475 \text{ ppm}$

d: both d_{bg} estimates from the same observation

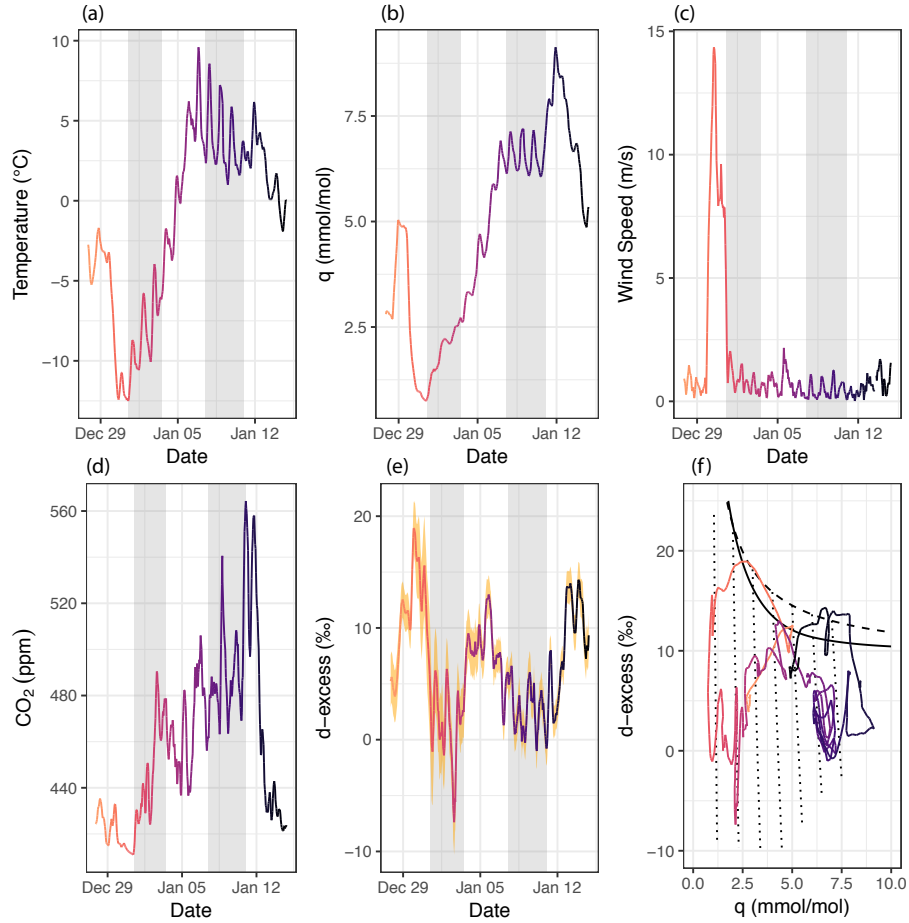


Figure 6. Relationship Relationships between meteorology, d-excess, and q (a) CO_2 from December 22, 2014–January 14, 2015. Time series of specific humidity–temperature (a, $^{\circ}\text{C}$), q , (b, mmol mol^{-1}), temperature–wind speed (c, m s^{-1}), and CO_2 –concentration CO_2 (d, ppm; 1σ uncertainty in orange shading) across, d-excess (e, ‰), and the relationship between dq vs q (f) spanning the same time period are shown for reference, with the same color gradient used across time in all four panels. Data are plotted as 6-hour running averages.

4.2.2 February 3-17, 2016

This period was marked by one extended PCAP from February 8 ~~12Z~~, 12 UTC to February 14, ~~12Z~~ 12 UTC (Fig. 7), and has been a major focus of recent air pollution studies (Baasandorj et al., 2017; Bares et al., 2018). Conditions prior to the PCAP were dry and cold for the first two days, before warming by $\sim 5^\circ\text{C}$ ~~and humidity increasing (Fig. 7a), concurrent with an~~
5 increase in humidity from ~ 3 to ~ 5 mmol mol⁻¹ (Fig. 7b~~).~~). Wind speeds peaked at the beginning of this period, and remained below 2 m s⁻¹ after February 5 (Fig. 7c). ~~CO₂-CO₂ increased from 430 to 480 ppm during this period before decreasing back to 430 ppm (Fig. 7d).~~ Deuterium excess also decreased ~~, but at a less rapid rate than anticipated for CDV addition, and instead,~~
10 by a few permil while CO₂ was elevated, but increased back to 3-5‰ until the beginning of the PCAP (Fig. 7e); humidity increased rapidly during this period, and followed a path parallel to moistening by ~~mixing addition~~ of “natural” ~~air masses~~
15 water vapor (Fig. 7a~~f~~). The remainder of the pre-PCAP period through the PCAP event was marked by slow, steady increases in q and ~~CO₂-CO₂~~, with prominent diurnal cycling in temperature, ~~CO₂-CO₂~~, q , and d-excess. Diurnal cyclicity was apparent in the relationship between d-excess and ~~CO₂-CO₂~~ as well, with periods of increasing (decreasing) ~~CO₂-CO₂~~ producing rapid decreases (increases) in d-excess with little change in q . These diurnal patterns are consistent with daytime growth of a shallow convective boundary layer at the surface with a stable layer aloft; the same interpretation was made in prior studies of this
20 event (Baasandorj et al., 2017). Diurnal cycle amplitudes of q , temperature, and ~~CO₂-CO₂~~ decreased for the second half of the PCAP (Fig. 7b-~~da~~, b, d), and co-occur with a reduction in surface solar radiation (~~Fig. 7e~~) as low-level clouds developed during the event. Superimposed on these diurnal cycles of d-excess against q , conditions became more moist across several days (Fig. 7a~~db~~, f). Following termination of the PCAP, conditions became warmer and ~~CO₂-CO₂~~ decreased back toward its background value. Humidity increased rapidly for a few days after the event before falling again. Both the moistening and
25 drying occurred with small changes in d-excess, consistent with changes expected for changes in q in the absence of the buildup of CDV. ~~Surface wind speeds remained low throughout this period (Fig. 7f), suggesting that removal of pollutants at the end of the PCAP was largely accomplished by vertical transport away from the surface.~~ In contrast to the previous case study, the relationship between d-excess and CO₂ excess is weak across this PCAP event (Table 2). Atmospheric soundings indicate the presence of a shallow convective mixed layer near the surface topped by a strong temperature inversion during this event
(e.g., Baasandorj et al., 2017), suggesting that the column within which CO₂ and CDV are emitted may larger than for PCAPs with high atmospheric stability lower in the column. Although changes in q across multiple days during this event seem to be driven by processes other than CDV addition, these observations support a strong CDV contribution on diurnal timescales as d-excess values and CO₂ concentrations are correlated at diurnal timescales but not necessarily multi-day timescales during this event.

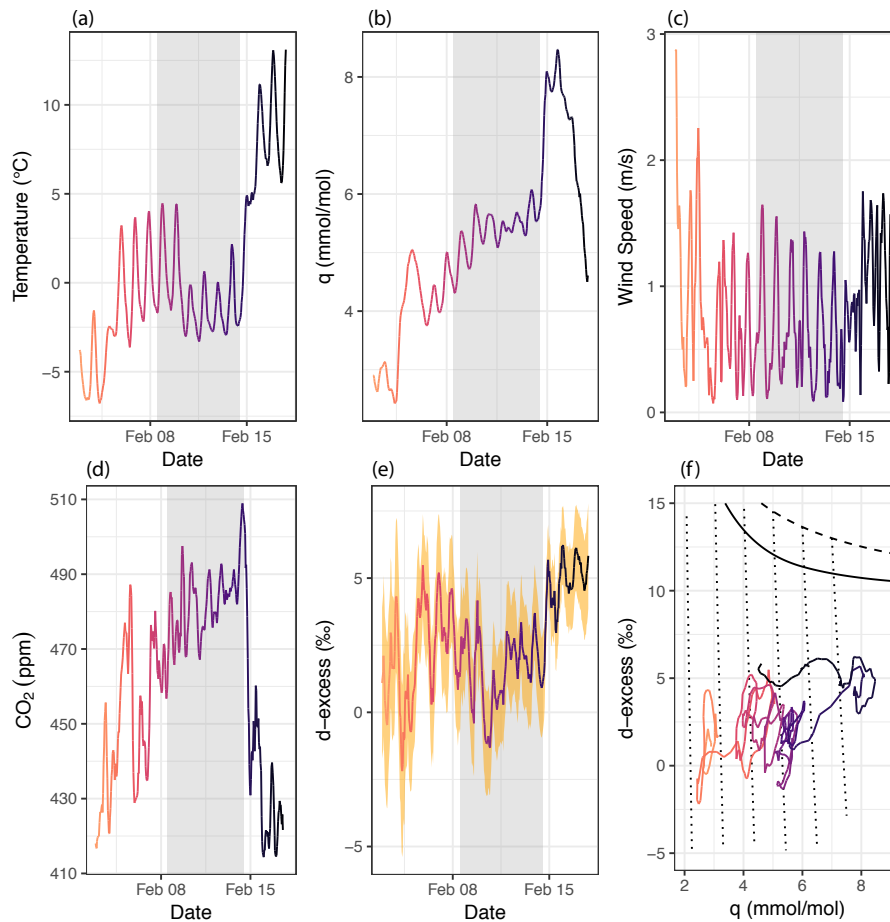


Figure 7. Relationship between d -excess and q (a) from February 1-17, 2016. Time series of specific humidity (b, mmol mol^{-1}), temperature (c, $^{\circ}\text{C}$), and CO_2 concentration (d, ppm; 1σ uncertainty in orange shading), d -excess (e, ‰), and the relationship between dq vs q (f) spanning the same time period, with the same color gradient used across time in all four panels. Data are plotted as 6-hour running averages.

4.2.3 December-25, 2016-January-10, 2017

4.3 Diurnal cycles of humidity, CO₂, and d-excess

Three separate PCAP events occurred during the December 25, 2016–January 10, 2017 period, at December 27 12Z to December 28 12Z, December 29 12Z to January 2 00Z, and January 7 12Z to January 8 12Z (Fig. ??). Initial conditions were humid (~ 7.5), with temperatures above zero and low CO₂ concentrations (Fig. ??b-d). Ahead of the first two PCAP events, temperature and humidity dropped (Fig. ??b,c), with an ~ 80 ppm increase in CO₂ following shortly after. Deuterium excess values decreased along with specific humidity prior to the first PCAP, but then decreased rapidly at the onset of the first PCAP with little change in specific humidity, likely a result of buildup in CDV associated with the increase in atmospheric CO₂ (Fig. ??a). The first and second PCAP events were separated by ~ 24 hours of decreased atmospheric stability, with a portion of the CO₂ buildup mixing out into the free troposphere (Fig. ??d). During this period, In this section, we more closely examine diurnal cycles of d-excess values increased as CDV was presumably diluted due to mixing. As the second PCAP started, CO₂ concentrations increased by ~ 100 , and d-excess values decreased by $\sim 10\%$. CO₂ fell through the latter half of the second PCAP, and mixed out to ~ 425 after the termination of the PCAP; during this period, d-excess increased by $>15\%$. Diurnal variability decreases throughout the second PCAP event, likely associated with the development of low-level clouds and a reduction of solar surface heating (Fig. ??e), as noted in prior events (Fig. 6,7) (Baasandorj et al., 2017; Whiteman et al., 2014). Humidity and temperatures decreased on January 5 with the passage of a second cold front, which had little impact on d-excess, but promoted strong surface cooling ahead of the third PCAP event. At the onset of the third PCAP, d-excess decreased by $>10\%$ and CO₂ increased by ~ 125 . As the third PCAP ended, surface temperature, humidity, and wind speeds all increased (Fig. ??b,e,f), while CO₂ decreased (Fig. ??d) and d-excess increased (Fig. ??a), consistent with pollutants being transported out of the SLV.

Relationship between d-excess and q (a) from December 25, 2016–January 10, 2017. Time series of specific humidity (b), temperature (c, °), and CO₂ concentration (d,) across the same time period are shown for reference, with the same color gradient used across time in all four panels. Data are plotted as 6-hour running averages.

4.4 Seasonal evolution of the diurnal cycle

CO₂, and specific humidity. We define diurnal cycles as deviations from the 24-hour running mean, and indicate them with a capital delta (Δ). Changes in the diurnal variability of the estimated mixing height and valley heat deficit were apparent throughout the winter season (Fig. 2). In this section, we investigate whether changes in the diurnal evolution of the mixed layer throughout the season were reflected in the ambient vapor isotope record of d-excess. Diurnal Despite subtle variation of the diurnal cycles of Δ d-excess and Δ CO₂ varied across years, months, and the presence or absence of a PCAP event, though CO₂, and Δq across years and months, several robust patterns emerged (Fig. 8). First, the shape of diurnal cycles of Δ d-excess and Δ CO₂ were consistent, though the magnitude and timing of changes varied across month, year, and valley stability status. Δ d-excess was flat or increased slightly in the early morning hours (0-6 MST Local Time, LT), decreased throughout the morning until ~ 11 MST LT, increased from 11 MST LT until late afternoon (~ 17 MST LT), and then decreased again from

17 MST-LT until late evening (Fig. 8a-i). Patterns in Δd -excess diurnal cycles mirrored ΔCO_2 patterns, cycle was $\sim 6\text{‰}$ during PCAP events (Fig. 8a), and closer to $\sim 3\text{‰}$ during non-PCAP periods (Fig. 8d).

Daily minimums in CO_2 - CO_2 mirror daily maximums in d-excess, and occurred during the period of the day expected to have the most developed boundary layer and greatest exchange between the near-surface atmosphere and the free troposphere surface and air aloft, is greatest (Fig. 8j-r). Broadly, the amplitude of these cycles was greater in January than in December and February and during PCAP events across the season. Across the entire time series (b,e). Conversely, daily minimums in Δd -excess occur when ΔCO_2 is increasing, likely reflecting the addition of CDV. Like Δd -excess, the amplitude of the d-excess and CO_2 diurnal cycles were $\sim 4\text{‰}$ and 30 respectively during January (diurnal cycle for ΔCO_2 is greater during PCAP periods (~ 40 ppm, Fig. 8b,k), but were closer to $\sim 3\text{‰}$ and 20-25 during December (l) than during non-PCAP periods (~ 20 ppm, Fig. 8a,j) and February (e). Patterns in Δd -excess diurnal cycles mirrored ΔCO_2 patterns, demonstrating the close association between d-excess and CO_2 on short time scales. In contrast, diurnal cycles of Δq show different patterns apart from amplitude across PCAP and non-PCAP periods (Fig. 8c,h). During PCAP events, average diurnal cycle amplitudes for d-excess and CO_2 increased to $\sim 6\text{‰}$ and >50 across all months periods, Δq increases from ~ 6 LT to ~ 18 LT, and decreases from ~ 18 LT to ~ 6 LT (Fig. 8d-fc), (m-o). Conversely, outside of PCAP events with an amplitude of $0.7\text{--}0.8$ mmol mol⁻¹ across the day. During non-PCAP periods, the amplitude of diurnal cycles decreased, presumably because CO_2 and CDV were mixed away from the surface more efficiently and therefore did not become concentrated near the surface.

the Δq diurnal cycle decreased to ~ 0.4 mmol mol⁻¹, and features a period stable humidity or slight humidity decrease during the afternoon, presumably due to greater mixing between the boundary layer and the free troposphere (Fig. 8f). Interannual variability in the diurnal cycles was generally small, with a few exceptions the largest differences observed during PCAP periods. For example, composite diurnal cycles for PCAP events varied the most across years (Fig. 8d-f, m-oa-c). However, given the episodic nature of PCAPs, these diurnal cycles can often be determined by 1 or 2 events in a given year. Though a consistent pattern emerged across many PCAP events, individual events were expressed differently in both the CO_2 - CO_2 and d-excess records (e.g., section 4.2). Nonetheless, the close associations between d-excess and CO_2 on diurnal cycles, coupled with the observation that these cycles are generally not coherent with changes in specific humidity, further suggest that the observed d-excess variability reflects the addition or removal of CDV.

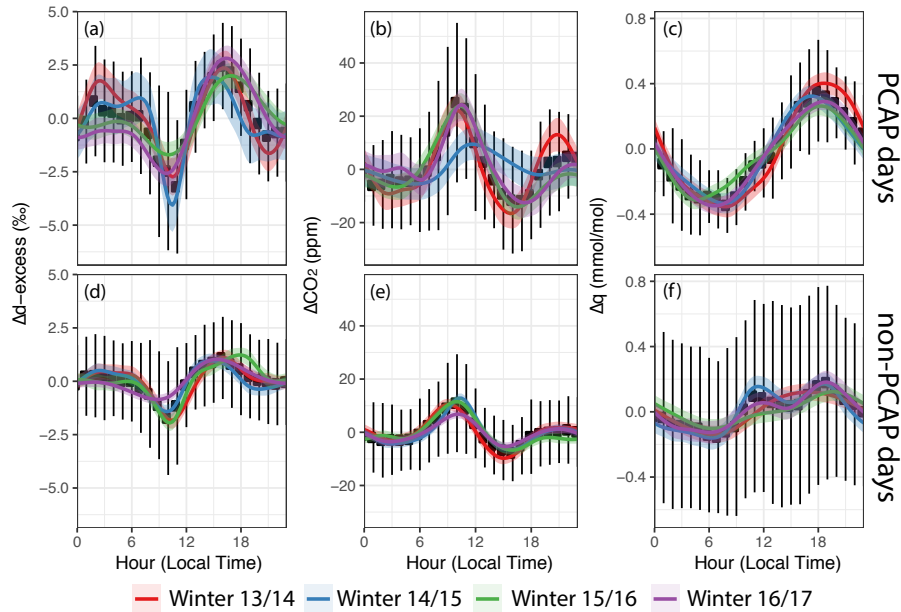


Figure 8. Diurnal seasonal average diurnal cycles of Δd -excess (top half left column) and ΔCO_2 - CO_2 (bottom half center column) by month. The left, center, and Δq (right column) correspond to December, January, and February. Within the top and bottom halves, there are three rows corresponding to all of the observational data, column for days in PCAP periods only, and conditions (top row) or non-PCAP periods only conditions (bottom row). Mean diurnal cycle (solid lines) and uncertainty (is approximated here as the standard error) deviation from a 24-hr moving average. Mean values across all four years are plotted shown as black symbols, with black vertical lines indicating 1σ variability. The mean diurnal cycle is modeled for each year independently as different colors, and are generated from a GAM using cubic cyclic smoothing splines. Diurnal cycles are modeled as the mean deviation between the hourly time series, and its 24-hour moving average. The influence of CDV in the diurnal cycle is apparent from comparing Δd -excess and CO_2 cycles: increases in CO_2 co-occur regression standard error shown as shaded ribbons, with decreases in d -excess during the early morning and late afternoon periods color corresponding to model year.

5 Discussion

CDV is evident across sub-diurnal to multi-day timescales in the Salt Lake City d-excess record. On short timescales, periods of high emission intensity ~~near or transport to the WBB~~ were apparent in the diurnal cycles of d-excess and $\text{CO}_2\text{-CO}_2$. Decreases in d-excess were coincident with increases in $\text{CO}_2\text{-CO}_2$, and occur during the morning and late afternoon when emissions were likely high and tropospheric mixing was low. Average diurnal cycles in d-excess and $\text{CO}_2\text{-CO}_2$ showed little change overnight outside of PCAP events (Fig. 8), which was unexpected as heating emissions continued throughout the evening. The absence of overnight d-excess and $\text{CO}_2\text{-CO}_2$ changes was likely a result of the ~~WBB-UOU's~~ location on a topographic bench away from large residential areas, or due to injection of cleaner air from above if a ~~SBI-surface-based inversion~~ occurs at an elevation below the ~~WBB-UOU site~~. Long-term records of CO_2 have also been collected in lower-elevation areas of the SLV and exhibit a greater buildup of CO_2 overnight during the winter than observed at UOU (Mitchell et al., 2018), which suggests that a stronger trend in nighttime d-excess and CO_2 values might be observed elsewhere in the SLV.

On longer timescales, the impact of CDV was most apparent during PCAP events, where $\text{CO}_2\text{-CO}_2$ and CDV persist in the urban atmosphere while the atmosphere in the SLV remained sufficiently stable. Some contrasts in the expression of CDV and $\text{CO}_2\text{-CO}_2$ were apparent across the winter season and likely resulted from changes in insolation and the mechanisms resulting in stability of the near-surface atmosphere. For example, the most rapid increases in $\text{CO}_2\text{-CO}_2$ and decreases in d-excess were observed during December and January (Fig. 3, 6, 7), when surface insolation was lower. In contrast, ~~rapid changes were less common during February, as a strong diurnal cycle but a more muted multi-day response was observed in February, when~~ higher insolation can drive higher mixing heights (Fig. 2) and mix out a greater proportion of daily emissions. As a result, changes in d-excess and $\text{CO}_2\text{-CO}_2$ exhibited large diurnal cycles superimposed upon slower synoptic trends during February PCAP events (Fig. 7).

Based on changes in d-excess relative to $\text{CO}_2\text{-CO}_2$ during PCAP events, and the HESTIA inventory of fossil fuel emissions for SLV (Patarasuk et al., 2016), we have estimated the mean d-excess of CDV to be ~~between -125% and -308%~~ $-179 \pm 17\%$. One assumption of the model used here is that all of the change in d-excess is driven by addition of CDV; other sources of vapor to the near surface, such as sublimation of snow or water evaporated from the Great Salt Lake, may introduce bias into these estimates. However, both of these sources would have less negative d-excess values, and therefore, if other sources of vapor contribute significantly to d-excess change, our estimates of d_{CDV} are a maximum estimate. ~~The wide range of estimated CDV compositions arises from uncertainties in the representative stoichiometric ratio between H_2O and CO_2 in combustion products (e.g., Deposition of vapor onto ice in supersaturated conditions can also promote a decrease in vapor d-excess (Galewsky et al., 2011; Jouzel and Merlivat, 1984). While we do not have any direct observations of supersaturated conditions, we cannot rule out the possibility of supersaturated conditions occurring when snow is in the valley or during cloud formation. However, we expect any potential role for vapor deposition under supersaturated conditions affecting vapor d-excess to be small, as we do not typically observe decreases in d-excess concurrent with decreases in specific humidity (Fig. 8).~~

We have made an estimate of 1.5 for ef . ~~In principle, ef can be constrained~~ through a detailed accounting of emissions or fuel sources from the HESTIA dataset (e.g., Patarasuk et al., 2016), but several sources of uncertainty in net ef remain.

For example, heat exchangers designed to improve heating efficiency may reduce the H_2O - H_2O concentration in emissions, and potentially alter d_{CDV} as well through condensation of water in the emissions stream (Fig. 1). Additionally, the portfolio of fuels contributing to CDV change in both time and space, and respond to meteorological conditions. For example, colder conditions increase demand for heating, which may shift the portfolio of fuel sources toward natural gas (e.g., Pataki et al., 2006). Finally, d_{CDV} can be altered by the temperature and degree of equilibration of ^{18}O between H_2O and CO_2 - H_2O and CO_2 in combustion exhaust. If no equilibration occurs between H_2O and CO_2 - H_2O and CO_2 , the $\delta^{18}\text{O}$ values of both species should be equal to atmospheric oxygen, 23.9‰ (Barkan and Luz, 2005; Gorski et al., 2015). In contrast, equilibration between H_2O and CO_2 - H_2O and CO_2 will lower the $\delta^{18}\text{O}$ value of H_2O - H_2O ; at 100° , for example, the $\delta^{18}\text{O}$ value of H_2O - H_2O will be $\sim 29\%$ lower than the $\delta^{18}\text{O}$ of CO_2 - CO_2 for complete equilibration (Friedman and O’Neil, 1977; Gorski et al., 2015). The degree of equilibration appeared to may vary across fuels and combustion systems (Horváth et al., 2012), which introduced introduces uncertainty into the $\delta^{18}\text{O}$, and subsequently d_{CDV} . Regardless, the highly negative estimated isotopic composition of the flux into the boundary layer during PCAP events, which we have assumed is predominantly CDV, precludes other potential sources of water vapor apart from CDV from explaining the observed isotopic change. Further refinements in CDV determination with stable water vapor isotopes may provide an additional tool with which to measure fossil fuel emissions and verify emissions reductions. These methods may also be helpful to verify that background CO_2 measurements are free from local emissions, as we would not expect to see a strong correlation between CO_2 concentrations and d-excess values in the absence of local emissions.

Though the most prominent periods of CO_2 - CO_2 and CDV buildup occur during PCAP events, decreases in d-excess coincident with increases in CO_2 were apparent across shorter timescales CO_2 were apparent outside of PCAPs as well. CO_2 and CDV from emissions built up in the boundary layer whenever atmospheric stability was present regardless of whether VHD values were high enough to qualify as a PCAP. For a given quantity of fuel burned, CO_2 - CO_2 increases and CDV concentrations will be higher if the mixed height is lower because the volume these species can mix into is smaller. Despite this, we saw no robust relationship between CDV or CO_2 and our mixing height estimates. Atmospheric soundings at the Salt Lake City airport occurred at 5 and 17 MST, however, LT, and were unlikely to capture diurnal extremes in the mixing height, confounding efforts to develop high-frequency relationships between mixing height, CO_2 , and CDV. Mid-afternoon patterns in the diurnal cycles of d-excess and CO_2 - CO_2 suggested that boundary layer development and entrainment did mix a fraction of combustion products out of the boundary layer. This pattern held even during PCAP events (Fig. 8a,b), though it is not clear whether this reflects mixing out of the valley, or just a repartitioning of pollutants within the atmospheric column below a capping inversion. In contrast, CO_2 - CO_2 and CDV build to higher concentrations during the early morning and late afternoon (Fig. 8), when boundary layer mixing was decreased and emissions were likely higher due to elevated traffic.

This technique for measuring water from combustion in urban areas can be adapted beyond the SLV, though different environments will present distinct challenges. The SLV is well-suited to detecting the buildup of CDV as it has a dry climate, features a large urban area in a topographic basin, and experiences frequent multi-day periods of high atmospheric stability in the winter. The CDV signal is largest in dry regions or during winter (Fig. 1), and CDV may comprise a larger fraction of urban humidity in these cities for a given level of emissions intensity. Additionally, CDV may have a larger impact

on the radiative balance of cities in drier regions, as longwave forcing increases logarithmically with water vapor amount (Raval and Ramanathan, 1989). However, though the CDV signal is higher at low humidities, instrumental precision is lower. Therefore, at current instrumental precision limits, there is a trade-off between precision of the CDV estimates and the size of the CDV signal. Based on our study, we suggest two potential refinements to this technique that will improve the accuracy and precision of this technique to diagnose the fraction of urban humidity arising from CDV. First, the largest source of known uncertainty in our estimates is associated with d_{CDV} . While our estimate of $-179 \pm 17\%$ is consistent with theoretical estimates, this fraction may vary through time as a result of changing fuel mixtures (affecting both isotopic composition and e/f) or measurement footprints, and has not been rigorously validated with direct measurements of d_{CDV} from a wide variety of fuel sources and combustion systems. Additionally, due to spatial variability in the δ^2H composition of fuels, d_{CDV} likely varies for other cities. Second, the estimate of the urban CDV fraction of humidity is highly sensitive to the estimate of d_{bg} . In this study, estimates of the CDV humidity percentage were 2.2% greater on average when a low CO_2 threshold was used rather than one based on the time window immediately preceding the PCAP; in one case, these assumptions yielded estimates that varied by a factor of 3.4, and in other cases, even yielded different signs (Table 3). In our uncertainty analysis, we have considered uncertainty arising from instrumental precision, but the uncertainty in d_{bg} remains difficult to assess. Paired urban-rural observations may be necessary to accurately estimate d_{bg} , or identify appropriate periods for estimating d_{bg} from the urban record.

6 Conclusions

Measurements of ambient vapor d-excess were paired with $\delta^{18}O_2$ - CO_2 observations across four winters in Salt Lake City, UT. We found a strong negative association between $\delta^{18}O_2$ - CO_2 and d-excess on sub-diurnal to seasonal timescales. Elevated $\delta^{18}O_2$ and CDV was most prominent during PCAP periods, where atmospheric stability was high for extended periods. We outline theoretical models that can discriminate between changes in d-excess driven by condensation, advection, and mixing processes the “natural” hydrological cycle and those driven by CDV moistening. CDV is most detectable. The CDV signal is largest when humidity is low, as CDV likely comprises a larger fraction of total humidity and the anticipated signal between vapor with and without CDV is large. Our estimates of -308 On shorter timescales, prominent diurnal cycles were observed in both d-excess and CDV that could be tied to both emissions intensity and atmospheric processes. These diurnal cycles were decoupled from diurnal cycles of specific humidity, further strengthening the link between d-excess and urban CO_2 .

We estimate the d-excess value of CDV to be $-179 \pm 17\%$ to -125% for d_{CDV} are assuming a mean molar ratio of $H_2O:CO_2$ in emissions of 1.5 derived from the HESTIA inventory of emissions for Salt Lake County (Patarasuk et al., 2016; Gurney et al., 2015), though the range remains large due to uncertainties in a uncertainty remains due to variability in the valley-scale stoichiometric ratio of H_2O and CO_2 and the degree of isotopic equilibration between H_2O and CO_2 in emissions. These estimated compositions, however, do suggest a significant role for CDV- H_2O and CO_2 and the measurement footprint, and uncertainties about the isotopic composition of fuels and their transit through different combustion systems. The latter of these uncertainties

can be reduced in future studies that seek to generate a "bottom-up" estimate of d_{CDV} from direct measurements of fuels and emissions vapor to complement the "top-down" estimate made in this study using a mixing-model approach. We use our d_{CDV} estimate to calculate the fraction of humidity in the SLV comprised of CDV using two different assumptions for the d-excess of water vapor in the absence of fossil fuel emissions. We find that CDV generally represents 5-10% of urban humidity during PCAP events, ~~particularly during periods where there was a large isotopic change, but little change in humidity. Prominent diurnal cycles were observed in both~~ with a maximum estimate of $16.7 \pm 3.2\%$. Estimates of urban CDV fraction require ~~an accurate estimate of the d-excess and CDV that could be tied to both emissions intensity and atmospheric processes of~~ water vapor in the absence of emissions, and we find generally higher estimates of urban CDV when a low- CO_2 threshold is used to estimate d_{bg} compared to when pre-PCAP observations alone are used. Further refinements of these methods may help apportion humidity changes during the winter between CDV and different advected "natural" water sources to the urban environment, and help verify ~~emissions amounts and/or emissions reductions that~~ CO_2 measurements that are taken as backgrounds are not influenced by local emissions. Additionally, our method is most immediately applicable to cities in arid or semi-arid areas during the winter, as the potential isotopic signal for detecting CDV is the largest. However, CDV may have the largest impact on urban meteorology when humidity is low, as greenhouse forcing by water vapor is logarithmically proportional to water vapor concentration. Further refinements of this humidity apportionment technique, such as narrowing the uncertainty in the isotopic composition of CDV and improving the estimation of d_{bg} will improve estimates of CDV amount in urban environments, and help assess relationships between CDV, CO_2 , urban air pollution, and public health.

Code and data availability. IGRA radiosonde data are available from

<https://www.ncdc.noaa.gov/data-access/weather-balloon/integrated-global-radiosonde-archive>. UOU meteorological measurements are available for download from mesowest.utah.edu, and CO_2 data are available at air.utah.edu. Calibrated UOU isotope data products are available from the Open Science Framework (osf.io/ekty3), and codes used to calibrate the water isotope analyzer measurements are available from GitHub (https://github.com/rfiorella/UU_vapor_processing_scripts/tree/v1.1.0)

Competing interests. The authors declare that they have no conflicts of interest.

Acknowledgements. RPF and GJB received support from NSF grant EF-1241286. RB, JCL, and the CO_2 measurements were supported by grants from Department of Energy (DOE) grant DESC0010624 and the National Oceanic and Atmospheric Administration (NOAA) grant NA140AR4310178.

References

- Andrews, A. E., Kofler, J. D., Trudeau, M. E., Williams, J. C., Neff, D. H., Masarie, K. A., Chao, D. Y., Kitzis, D. R., Novelli, P. C., Zhao, C. L., Dlugokencky, E. J., Lang, P. M., Crotwell, M. J., Fischer, M. L., Parker, M. J., Lee, J. T., Baumann, D. D., Desai, A. R., Stanier, C. O., De Wekker, S. F. J., Wolfe, D. E., Munger, J. W., and Tans, P. P.: CO₂, CO, and CH₄ measurements from tall towers in the NOAA earth system research laboratory's global greenhouse gas reference network: Instrumentation, uncertainty analysis, and recommendations for future high-accuracy greenhouse gas monitoring efforts, *Atmospheric Measurement Techniques*, 7, 647–687, <https://doi.org/10.5194/amt-7-647-2014>, 2014.
- Baasandorj, M., Hoch, S. W., Bares, R., Lin, J. C., Brown, S. S., Millet, D. B., Martin, R., Kelly, K., Zarzana, K. J., Whiteman, C. D., Dube, W. P., Tonnesen, G., Jaramillo, I. C., and Sohl, J.: Coupling between Chemical and Meteorological Processes under Persistent Cold-Air Pool Conditions: Evolution of Wintertime PM_{2.5} Pollution Events and N₂O₅ Observations in Utah's Salt Lake Valley, *Environmental Science and Technology*, 51, 5941–5950, <https://doi.org/10.1021/acs.est.6b06603>, 2017.
- Bares, R., Lin, J. C., Hoch, S. W., Baasandorj, M., Mendoza, D., Fasoli, B., Mitchell, L., and Stephens, B. B.: The wintertime co-variation of CO₂ and criteria pollutants in an urban valley of the Western US, *Journal of Geophysical Research Atmospheres*, 123, <https://doi.org/10.1002/2017JD027917>, 2018.
- Barkan, E. and Luz, B.: High precision measurements of 17O/16O and 18O/16O ratios in H₂O, *Rapid Communications in Mass Spectrometry*, 19, 3737–3742, <https://doi.org/10.1002/rcm.2250>, 2005.
- Bergeron, O. and Strachan, I. B.: Wintertime radiation and energy budget along an urbanization gradient in Montreal, Canada, *International Journal of Climatology*, 32, 137–152, <https://doi.org/10.1002/joc.2246>, 2012.
- Blossey, P. N., Kuang, Z., and Romps, D. M.: Isotopic composition of water in the tropical tropopause layer in cloud-resolving simulations of an idealized tropical circulation, *Journal of Geophysical Research Atmospheres*, 115, 1–23, <https://doi.org/10.1029/2010JD014554>, 2010.
- Bony, S., Risi, C., and Vimeux, F.: Influence of convective processes on the isotopic composition ($\delta^{18}\text{O}$ and δD) of precipitation and water vapor in the tropics: 1. Radiative-convective equilibrium and Tropical Ocean-Global Atmosphere-Coupled Ocean-Atmosphere Response Experiment (TOGA-COARE), *Journal of Geophysical Research Atmospheres*, 113, 1–21, <https://doi.org/10.1029/2008JD009942>, 2008.
- Bradley, R. S., Keimig, F. T., and Diaz, H. F.: Recent Changes in the North American Arctic Boundary Layer in Winter, <https://doi.org/10.1029/93JD00311>, 1993.
- Brook, R. D., Rajagopalan, S., Pope, C. A., Brook, J. R., Bhatnagar, A., Diez-Roux, A. V., Holguin, F., Hong, Y., Luepker, R. V., Mittleman, M. A., Peters, A., Siscovick, D., Smith, S. C., Whitsel, L., and Kaufman, J. D.: Particulate matter air pollution and cardiovascular disease: An update to the scientific statement from the american heart association, *Circulation*, 121, 2331–2378, <https://doi.org/10.1161/CIR.0b013e3181dbee1>, 2010.
- Carlton, A. G. and Turpin, B. J.: Particle partitioning potential of organic compounds is highest in the Eastern US and driven by anthropogenic water, *Atmospheric Chemistry and Physics*, 13, 10 203–10 214, <https://doi.org/10.5194/acp-13-10203-2013>, 2013.
- Dabelstein, W., Reglitzky, A., Schütze, A., and Reders, K.: Automotive Fuels, in: *Ullmann's Encyclopedia of Industrial Chemistry*, vol. 4, pp. 423–458, Wiley-VCH Verlag GmbH & Co. KGaA, Weinheim, https://doi.org/10.1002/14356007.a16_719.pub2, 2012.
- Dansgaard, W.: Stable isotopes in precipitation, *Tellus*, 16, 436–468, <https://doi.org/10.3402/tellusa.v16i4.8993>, <https://www.tandfonline.com/doi/full/10.3402/tellusa.v16i4.8993>, 1964.
- Dockery, D. and Pope, A.: Acute Respiratory Effects of Particulate Air Pollution., *Annual Review of Public Health*, 15, 107–132, <https://doi.org/10.1146/annurev.pu.15.050194.000543>, 1994.

- Duren, R. M. and Miller, C. E.: Measuring the carbon emissions of megacities, *Nature Climate Change*, 2, 560–562, <https://doi.org/10.1038/nclimate1629>, <http://dx.doi.org/10.1038/nclimate1629>, 2012.
- Durre, I. and Yin, X.: Enhanced radiosonde data for studies of vertical structure, *Bulletin of the American Meteorological Society*, 89, 1257–1261, <https://doi.org/10.1175/2008BAMS2603.1>, 2008.
- 5 EIA, U.: State Carbon Dioxide Emissions Data, Tech. rep., 2015.
- Estep, M. F. and Hoering, T. C.: Biogeochemistry of the stable hydrogen isotopes, *Geochimica et Cosmochimica Acta*, 44, 1197–1206, [https://doi.org/10.1016/0016-7037\(80\)90073-3](https://doi.org/10.1016/0016-7037(80)90073-3), <http://www.sciencedirect.com/science/article/pii/0016703780900733>, 1980.
- Fiorella, R. P., Poulsen, C. J., Zolá, R. S. P., Jeffery, M. L., and Ehlers, T. A.: Modern and long-term evaporation of central Andes surface waters suggests paleo archives underestimate Neogene elevations, *Earth and Planetary Science Letters*, 432, 59–72, <https://doi.org/10.1016/j.epsl.2015.09.045>, www.elsevier.com/locate/epsl, 2015.
- 10 Friedman, I. and O’Neil, J. R.: Data of geochemistry: Compilation of stable isotope fractionation factors of geochemical interest, vol. 440, US Government Printing Office, 1977.
- Galewsky, J., Rella, C., Sharp, Z., Samuels, K., and Ward, D.: Surface measurements of upper tropospheric water vapor isotopic composition on the Chajnantor Plateau, Chile, *Geophysical Research Letters*, 38, 1–5, <https://doi.org/10.1029/2011GL048557>, 2011.
- 15 Gat, J. R.: Oxygen and Hydrogen Isotopes in the Hydrologic Cycle, *Annual Review of Earth and Planetary Sciences*, 24, 225–262, <https://doi.org/10.1146/annurev.earth.24.1.225>, <http://www.annualreviews.org/doi/10.1146/annurev.earth.24.1.225>, 1996.
- Gillies, R. R., Wang, S.-Y., Yoon, J.-H., and Weaver, S.: CFS Prediction of Winter Persistent Inversions in the Intermountain Region, *Weather and Forecasting*, 25, 1211–1218, <https://doi.org/10.1175/2010WAF2222419.1>, <http://journals.ametsoc.org/doi/abs/10.1175/2010WAF2222419.1>, 2010.
- 20 Gorski, G., Strong, C., Good, S. P., Bares, R., Ehleringer, J. R., and Bowen, G. J.: Vapor hydrogen and oxygen isotopes reflect water of combustion in the urban atmosphere., *Proceedings of the National Academy of Sciences of the United States of America*, 112, 3247–52, <https://doi.org/10.1073/pnas.1424728112>, <http://www.pnas.org/content/112/11/3247.short>, 2015.
- Green, M. C., Chow, J. C., Watson, J. G., Dick, K., and Inouye, D.: Effects of snow cover and atmospheric stability on winter PM_{2.5} concentrations in western U.S. Valleys, *Journal of Applied Meteorology and Climatology*, 54, 1191–1201, <https://doi.org/10.1175/JAMC-D-14-0191.1>, 2015.
- 25 Gurney, K. R., Razlivanov, I., Song, Y., Zhou, Y., Benes, B., and Abdul-Massih, M.: Quantification of Fossil Fuel CO₂ Emissions on the Building/Street Scale for a Large U.S. City, *Environmental Science & Technology*, 46, 12 194–12 202, <https://doi.org/10.1021/es3011282>, 2012.
- Holmer, B. and Eliasson, I.: Urban-rural vapour pressure differences and their role in the development of urban heat islands, *International Journal of Climatology*, 19, 989–1009, 1999.
- 30 Horel, J., Splitt, M., Dunn, L., Pechmann, J., White, B., Ciliberti, C., Lazarus, S., Slemmer, J., Zaff, D., and Burks, J.: MesoWest: Cooperative mesonets in the western United States, *Bulletin of the American Meteorological Society*, 83, 211–225, [https://doi.org/10.1175/1520-0477\(2002\)083<0211:MCMITW>2.3.CO;2](https://doi.org/10.1175/1520-0477(2002)083<0211:MCMITW>2.3.CO;2), 2002.
- Horita, J. and Wesolowski, D. J.: Liquid-vapor fractionation of oxygen and hydrogen isotopes of water from the freezing to the critical temperature, *Geochimica et Cosmochimica Acta*, 58, 3425–3437, [https://doi.org/10.1016/0016-7037\(94\)90096-5](https://doi.org/10.1016/0016-7037(94)90096-5), 1994.
- 35 Horváth, B., Hofmann, M., and Pack, A.: On the triple oxygen isotope composition of carbon dioxide from some combustion processes, *Geochimica et Cosmochimica Acta*, 95, 160–168, <https://doi.org/10.1016/j.gca.2012.07.021>, <http://linkinghub.elsevier.com/retrieve/pii/S0016703712004139>, 2012.

- Jouzel, J. and Merlivat, L.: Deuterium and oxygen 18 in precipitation: Modeling of the isotopic effects during snow formation, *Journal of Geophysical Research*, 89, 11 749, <https://doi.org/10.1029/JD089iD07p11749>, 1984.
- Kaufman, Y. J. and Koren, I.: Smoke and Pollution Aerosol Effect on Cloud Cover, *Science*, 313, 655–658, <https://doi.org/10.1126/science.1126232>, 2006.
- 5 Keeling, C. D.: The concentration and isotopic abundances of atmospheric carbon dioxide in rural areas, *Geochimica et Cosmochimica Acta*, 13, 322–334, 1958.
- Keeling, C. D.: The concentration and isotopic Abundances of Carbon Dioxide in rural and marine air, *Geochimica et Cosmochimica Acta*, 24, 277–298, 1961.
- Kourtidis, K., Stathopoulos, S., Georgoulas, A. K., Alexandri, G., and Rapsomanikis, S.: A study of the impact of synoptic weather conditions and water vapor on aerosol-cloud relationships over major urban clusters of China, *Atmospheric Chemistry and Physics*, 15, 10 955–10 964, <https://doi.org/10.5194/acp-15-10955-2015>, 2015.
- 10 Lareau, N. P., Crosman, E., Whiteman, C. D., Horel, J. D., Hoch, S. W., Brown, W. O. J., and Horst, T. W.: The persistent cold-air pool study, *Bulletin of the American Meteorological Society*, 94, 51–63, <https://doi.org/10.1175/BAMS-D-11-00255.1>, 2013.
- Le Quééré, C., Andrew, R. M., Friedlingstein, P., Sitch, S., Pongratz, J., and Korsbakken, Glen P. Peters, Josep G. Canadell, Robert B. Jackson, Thomas A. Boden, Pieter P. Tans, Oliver D. Andrews, Vivek Arora, Dorothee C. E. Bakker, Leticia Barbero, Meike Becker, Richard A. Betts, Laurent Bopp, Frédéric Chevallier, Louise P. Chini., D. Z. Z.: The Global Carbon Budget 2017, *Earth Syst. Sci. Data*, 10, 405–448, <https://doi.org/https://doi.org/10.5194/essdd-2017-123>, 2018.
- 15 Majoube, M.: Fractionation factor of ^{18}O between water vapour and ice, *Nature*, 226, 1242, 1970.
- Malek, E., Davis, T., Martin, R. S., and Silva, P. J.: Meteorological and environmental aspects of one of the worst national air pollution episodes (January, 2004) in Logan, Cache Valley, Utah, USA, *Atmospheric Research*, 79, 108–122, <https://doi.org/10.1016/j.atmosres.2005.05.003>, 2006.
- 20 McCarthy, M. P., Best, M. J., and Betts, R. A.: Climate change in cities due to global warming and urban effects, *Geophysical Research Letters*, 37, 1–5, <https://doi.org/10.1029/2010GL042845>, 2010.
- Merlivat, L. and Nief, G.: Isotopic fractionation of solid-vapor and liquid-vapor changes of state of water at temperatures below 0°C , *Tellus*, 19, 122–127, 1967.
- 25 Miller, J. B. and Tans, P. P.: Calculating isotopic fractionation from atmospheric measurements at various scales, *Tellus, Series B: Chemical and Physical Meteorology*, 55, 207–214, <https://doi.org/10.1034/j.1600-0889.2003.00020.x>, 2003.
- Mitchell, L. E., Lin, J., Bowling, D., Pataki, D., Strong, C., Schauer, A., Bares, R., Bush, S., Stephens, B., Mendoza, D., Mallia, D., Holland, L., Gurney, K., and Ehleringer, J.: Long-term urban carbon dioxide observations reveal spatial and temporal dynamics related to urban characteristics and growth, *Proceedings of the National Academy of Sciences*, 2018.
- 30 Mölders, N. and Olson, M. A.: Impact of Urban Effects on Precipitation in High Latitudes, *J. Hydrometeor*, 5, 409–429, [https://doi.org/http://dx.doi.org/10.1175/1525-7541\(2004\)005<0409:IOUEOP>2.0.CO;2](https://doi.org/http://dx.doi.org/10.1175/1525-7541(2004)005<0409:IOUEOP>2.0.CO;2), [http://journals.ametsoc.org/doi/abs/10.1175/1525-7541\(2004\)005\(0409:IOUEOP\)3E2.0.CO;2](http://journals.ametsoc.org/doi/abs/10.1175/1525-7541(2004)005(0409:IOUEOP)3E2.0.CO;2), 2004.
- Morris, R., Naumova, E. N., and Munasinghe, R. L.: Ambient air pollution and hospitalization for congestive heart failure among elderly people in seven large U.S. cities, *American Journal of Public Health*, 85, 1361–1365, <https://doi.org/10.2105/AJPH.85.10.1361>, 1995.
- 35 Pataki, D. E., Bowling, D., and Ehleringer, J.: Seasonal cycle of carbon dioxide and its isotopic composition in an urban atmosphere: Anthropogenic and biogenic effects, *Journal of Geophysical Research*, 108, 1–8, <https://doi.org/10.1029/2003JD003865>, 2003.

- Pataki, D. E., Tyler, B. J., Peterson, R. E., Nair, A. P., Steenburgh, W. J., and Pardyjak, E. R.: Can carbon dioxide be used as a tracer of urban atmospheric transport?, *Journal of Geophysical Research D: Atmospheres*, 110, 1–8, <https://doi.org/10.1029/2004JD005723>, 2005.
- Pataki, D. E., Bowling, D. R., Ehleringer, J. R., and Zobitz, J. M.: High resolution atmospheric monitoring of urban carbon dioxide sources, *Geophysical Research Letters*, 33, 1–5, <https://doi.org/10.1029/2005GL024822>, 2006.
- 5 Pataki, D. E., Xu, T., Luo, Y. Q., and Ehleringer, J. R.: Inferring biogenic and anthropogenic carbon dioxide sources across an urban to rural gradient, *Oecologia*, 152, 307–322, <https://doi.org/10.1007/s00442-006-0656-0>, 2007.
- Patarasuk, R., Gurney, K. R., O’Keeffe, D., Song, Y., Huang, J., Rao, P., Buchert, M., Lin, J. C., Mendoza, D., and Ehleringer, J. R.: Urban high-resolution fossil fuel CO₂ emissions quantification and exploration of emission drivers for potential policy applications, *Urban Ecosystems*, 19, 1013–1039, <https://doi.org/10.1007/s11252-016-0553-1>, <http://dx.doi.org/10.1007/s11252-016-0553-1>, 2016.
- 10 Pruppacher, H. and Klett, J.: *Microphysics of Clouds and Precipitation*, Springer Netherlands, 2 edn., <https://doi.org/10.1007/978-0-306-48100-0>, 2010.
- Raval, A. and Ramanathan, V.: Observational determination of the greenhouse effect, *Nature*, 342, 758–761, <https://doi.org/10.1038/340301a0>, <http://www.nature.com/doi/finder/10.1038/340301a0>, 1989.
- Rosenfeld, D., Lohmann, U., Raga, G. B., O’Dowd, C. D., Kulmala, M., Fuzzi, S., Reissell, A., and Andreae, M. O.: Flood or drought: How do aerosols affect precipitation?, *Science*, 321, 1309–1313, <https://doi.org/10.1126/science.1160606>, 2008.
- 15 Rozanski, K., Araguás-Araguás, L., and Gonfiantini, R.: Isotopic Patterns in Modern Global Precipitation, in: *Climate Change in Continental Isotopic Records*, edited by Swart, P. K., Lohmann, K. C., McKenzie, J., and Savin, S. M., pp. 1–36, American Geophysical Union, Washington, DC, 1993.
- Sailor, D. J.: A review of methods for estimating anthropogenic heat and moisture emissions in the urban environment, *International Journal of Climatology*, 31, 189–199, <https://doi.org/10.1002/joc.2106>, 2011.
- 20 Salmon, O. E., Shepson, P. B., Ren, X., Marquardt Collow, A. B., Miller, M. A., Carlton, A. G., Cambaliza, M. O., Heimburger, A., Morgan, K. L., Fuentes, J. D., Stirm, B. H., Grundman, R., and Dickerson, R. R.: Urban emissions of water vapor in winter, *Journal of Geophysical Research: Atmospheres*, 122, 9467–9484, <https://doi.org/10.1002/2016JD026074>, 2017.
- Schobert, H. H.: *Chemistry of Fossil Fuels and Biofuels*, 2013.
- 25 Seidel, D. J., Zhang, Y., Beljaars, A., Golaz, J.-C., Jacobson, A. R., and Medeiros, B.: Climatology of the planetary boundary layer over the continental United States and Europe, *Journal of Geophysical Research: Atmospheres*, 117, n/a–n/a, <https://doi.org/10.1029/2012JD018143>, <http://doi.wiley.com/10.1029/2012JD018143>, 2012.
- Sessions, A. L., Burgoyne, T. W., Schimmelmann, A., and Hayes, J. M.: Fractionation of hydrogen isotopes in lipid biosynthesis, *Organic Geochemistry*, 30, 1193–1200, [https://doi.org/10.1016/S0146-6380\(99\)00094-7](https://doi.org/10.1016/S0146-6380(99)00094-7), 1999.
- 30 Strong, C., Stwertka, C., Bowling, D. R., Stephens, B. B., and Ehleringer, J. R.: Urban carbon dioxide cycles within the Salt Lake Valley: A multiple-box model validated by observations, *Journal of Geophysical Research Atmospheres*, 116, 1–12, <https://doi.org/10.1029/2011JD015693>, 2011.
- Trenberth, K. E., Fasullo, J., Smith, L., Qian, T., and Dai, A.: Estimates of the Global Water Budget and Its Annual Cycle Using Observational and Model Data, *Journal of hydrometeorology - special section*, 8, 758–769, <https://doi.org/10.1175/JHM600.1>, 2006.
- 35 Twohy, C. H., Coakley, J. A., and Tahnk, W. R.: Effect of changes in relative humidity on aerosol scattering near clouds, *Journal of Geophysical Research Atmospheres*, 114, 1–12, <https://doi.org/10.1029/2008JD010991>, 2009.
- Vogelezang, D. H. P. and Holtzlag, A. A. M.: Evaluation and model impacts of alternative boundary-layer height formulations, *Boundary-Layer Meteorology*, 81, 245–269, 1996.

- Webster, C. R. and Heymsfield, A. J.: Water isotope ratios D/H, 18O/16O, 17O/16O in and out of clouds map dehydration pathways., *Science*, 302, 1742–1745, <https://doi.org/10.1126/science.1089496>, 2003.
- Whiteman, C. D., Bian, X., and Zhong, S.: Wintertime evolution of the temperature inversion in the Colorado Plateau Basin, *Journal of Applied Meteorology*, 38, 1103–1117, [https://doi.org/10.1175/1520-0450\(1999\)038<1103:WEOTTI>2.0.CO;2](https://doi.org/10.1175/1520-0450(1999)038<1103:WEOTTI>2.0.CO;2), 1999.
- 5 Whiteman, C. D., Zhong, S., Shaw, W. J., Hubbe, J. M., Bian, X., and Mittelstadt, J.: Cold Pools in the Columbia Basin, *Weather and Forecasting*, 16, 432–447, [https://doi.org/10.1175/1520-0434\(2001\)016<0432:CPITCB>2.0.CO;2](https://doi.org/10.1175/1520-0434(2001)016<0432:CPITCB>2.0.CO;2), 2001.
- Whiteman, C. D., Hoch, S. W., Horel, J. D., and Charland, A.: Relationship between particulate air pollution and meteorological variables in Utah’s Salt Lake Valley, *Atmospheric Environment*, 94, 742–753, <https://doi.org/10.1016/j.atmosenv.2014.06.012>, 2014.
- Zhao, C. L. and Tans, P. P.: Estimating uncertainty of the WMO mole fraction scale for carbon dioxide in air, *Journal of Geophysical Research*
- 10 *Atmospheres*, 111, 1–10, <https://doi.org/10.1029/2005JD006003>, 2006.
- Zhou, Y. and Gurney, K.: A new methodology for quantifying on-site residential and commercial fossil fuel CO ₂ emissions at the building spatial scale and hourly time scale, *Carbon Management*, 1, 45–56, <https://doi.org/10.4155/cmt.10.7>, <http://www.tandfonline.com/doi/abs/10.4155/cmt.10.7>, 2010.